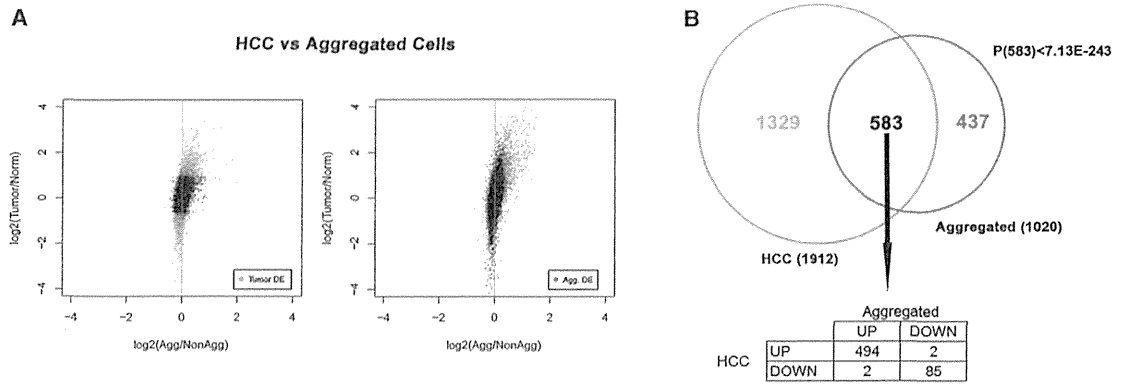

C

	UPREGULATED GENES			DOWNREGULATED GENES		
	AGGREGATED		HCC	AGGREGATED		HCC
BIOLOGICAL PROCESS	immune system process	9.05E-10	vasculature development	1.69E-09	metabolic process	4.81E-11	oxidation reduction	2.80E-51
	vasculature development	4.76E-08	blood vessel development	2.47E-09	cellular ketone metabolic process	2.33E-08	metabolic process	6.14E-39
	immune response	4.92E-08	angiogenesis	7.41E-09	oxidation reduction	3.59E-08	cellular ketone metabolic process	1.76E-35
	blood vessel development	9.17E-08	blood vessel morphogenesis	6.77E-08	carboxylic acid metabolic process	5.46E-08	oxoacid metabolic process	5.27E-35
	system development	1.53E-07	cell adhesion	1.13E-07	oxoacid metabolic process	5.46E-08	carboxylic acid metabolic process	5.27E-35
	response to external stimulus	5.22E-07	biological adhesion	1.22E-07	organic acid metabolic process	5.76E-08	organic acid metabolic process	6.44E-35
	anatomical structure development	1.08E-06	regulation of developmental process	2.10E-07	cellular metabolic process	5.49E-07	monocarboxylic acid metabolic process	6.63E-22
	regulation of multicellular organismal process	1.88E-06	response to external stimulus	4.23E-07	cofactor metabolic process	2.96E-04	cellular metabolic process	2.41E-18
	multicellular organismal development	2.34E-06	regulation of multicellular organismal process	3.24E-06	coenzyme metabolic process	4.66E-04	organic acid catabolic process	6.12E-16
	response to wounding	2.51E-06	response to wounding	3.44E-05	cellular amine metabolic process	1.43E-03	carboxylic acid catabolic process	6.12E-16
CELLULAR COMPONENT	extracellular region part	6.50E-20	extracellular region part	4.80E-14	intracellular part	3.51E-18	mitochondrion	5.70E-83
	extracellular region	5.46E-15	extracellular matrix	1.81E-10	intracellular	4.69E-17	cytoplasm	2.43E-57
	plasma membrane	2.49E-10	plasma membrane	2.64E-10	cytoplasm	6.98E-16	cytoplasmic part	9.43E-49
	proteinaceous extracellular matrix	3.76E-10	proteinaceous extracellular matrix	3.81E-10	mitochondrion	1.08E-12	intracellular part	1.58E-48
	extracellular matrix	3.96E-10	membrane	1.41E-09	cytoplasmic part	6.09E-11	intracellular membrane-bounded organelle	6.50E-47
	extracellular space	5.39E-10	extracellular region	1.68E-09	intracellular membrane-bounded organelle	1.16E-10	membrane-bounded organelle	8.96E-47
	cell surface	1.75E-07	lysosome	2.55E-09	membrane-bounded organelle	1.27E-10	intracellular	6.19E-44
	plasma membrane part	1.00E-06	endoplasmic reticulum	2.63E-09	intracellular organelle	1.23E-09	mitochondrial part	8.61E-42
	external side of plasma membrane	1.57E-06	lytic vacuole	3.08E-09	organelle	1.31E-09	intracellular organelle	3.77E-35
	lysosome	1.32E-05	plasma membrane part	2.16E-08	mitochondrial part	1.77E-03	organelle	4.53E-35

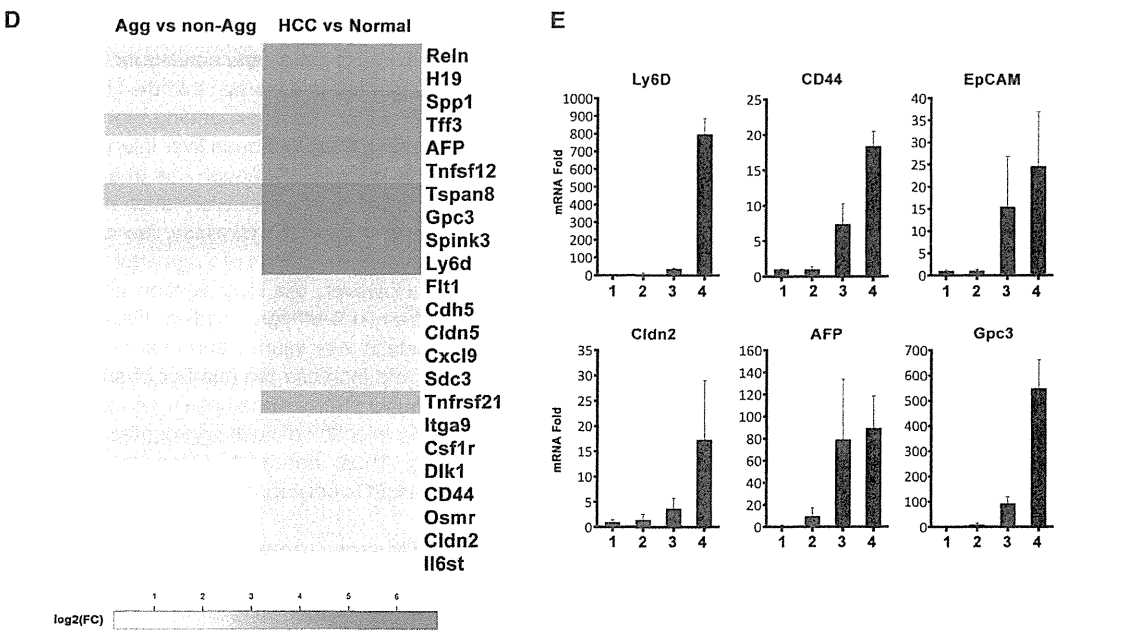

Figure 3. Aggregated Hepatocytes Exhibit an Altered Transcriptome Similar to that of HCC Cells

Aggregated and matched nonaggregated hepatocytes were isolated 5 months after DEN treatment. HCC cells were isolated from DEN-induced tumors, and normal hepatocytes were from age- and gender-matched control mice. RNA was extracted and subjected to microarray analysis (n = 3 for each sample).

(A) Scatterplot representing fold changes (log 2 of expression ratio) in gene expression for HCC versus normal (y axis) and aggregated versus nonaggregated (x axis) pairwise transcriptome comparisons. The plot is displayed twice: in the left panel, genes with an FDR < 0.01 in the aggregated versus nonaggregated

(legend continued on next page)

hepatocyte samples did not cluster with each other but rather with nonaggregated hepatocytes derived from the same mouse (Figure S3A). Interestingly, the aggregated cell transcriptome appeared closer to that of normal hepatocytes than to the HCC profile. This similarity may be due to the presence of ~70% nontumorigenic (or $CD44^-$) hepatocytes within the purified aggregates (Figure 1D). Comparison of the HCC and normal hepatocyte transcriptomes revealed 1,912 differentially expressed genes (false discovery rate [FDR] < 0.01; Figure 3A, left, cyan dots). A similar comparison revealed 1,020 genes that are differentially expressed between aggregated and nonaggregated hepatocytes (FDR < 0.01; Figure 3A, right, red dots). The range of differential expression is wider for the HCC and normal hepatocyte pair than the aggregate versus nonaggregate pair, reflecting presence of normal, nontransformed hepatocytes within the aggregates, resulting in signal dilution. Interestingly, 57% (583/1,020) of genes differentially expressed in aggregated relative to nonaggregated hepatocytes are also differentially expressed in HCC relative to normal hepatocytes (Figure 3B, top), a value that is highly significant ($p < 7.13 \times 10^{-243}$). More specifically, 85% (494/583) of these genes are overexpressed in both HCC and HcPC-containing aggregates (Figure 3B, bottom table). Thus, hepatocyte aggregates isolated 5 months after DEN injection contain cells that are related in their gene expression profile to HCC cells isolated from fully developed tumor nodules.

To gain insight into the functional differences between the transcriptomes of the four populations, we examined which biological processes or cellular compartments were significantly overrepresented in the induced or repressed genes in both pairwise comparisons (Gene Ontology Analysis). As expected, processes and compartments that were enriched in aggregated hepatocytes relative to nonaggregated hepatocytes were almost identical to those that were enriched in HCC relative to normal hepatocytes (Figure 3C). Upregulated genes were related to immune response, angiogenesis, development, and wound healing, and many encoded plasma membrane or secreted proteins. By contrast, downregulated genes were highly enriched for metabolic processes, and many of them encoded mitochondrial proteins or had functions associated with differentiated hepatocytes (Figure 3C). Several human HCC markers, including AFP, Gpc3 and H19, were upregulated in aggregated hepatocytes (Figures 3D and 3E). Aggregated hepatocytes also expressed more Tetraspanin 8 (Tspan8), a cell-surface glycoprotein that complexes with integrins and is overexpressed in human carcinomas (Zöller, 2009). Another cell-surface molecule highly expressed in aggregated cells is Ly6D (Figures 3D and 3E). Immunofluorescence (IF) analysis revealed that Ly6D was undetectable in normal liver but was elevated in FAH and ubiquitously expressed in most HCC cells (Figure S3C). A fluorescent-labeled Ly6D antibody injected into HCC-bearing mice specifically stained tumor nodules (Figure S3D). Other cell-surface molecules that were upregulated in aggregated cells included syndecan 3 (Sdc3), integrin α 9 (Itga9), claudin 5 (Cldn5), and cadherin 5 (Cdh5) (Figure 3D). Aggregated hepatocytes also exhibited elevated expression of extracellular matrix proteins (TIF3 and Reln1) and a serine protease inhibitor (Spink3). Elevated expression of such proteins may explain aggregate formation. Aggregated hepatocytes also expressed progenitor cell markers, including the epithelial cell adhesion molecule (EpCAM) (Figure 3E) and Dlk1 (Figure 3D). Elevated expression of cytokines and cytokine receptors was also detected, including tumor necrosis factor superfamily members 12 and 21, colony-stimulating factor 1 receptor, FMS-like tyrosine kinase 1, chemokine (C-X-C motif) ligand 9, the STAT3-activating cytokine osteopontin, IL-6 receptor (IL-6R) signal transducing subunit (gp130), and oncostatin M (OSM) receptor, which also activates STAT3 (Figure 3D).

Aggregated hepatocytes expressed albumin, albeit less than nonaggregated hepatocytes (Figure 4A). Some aggregated cells were positive for cytokeratin 19 (CK19) and A6, markers for bile duct epithelium and oval cells (Figure 4A). Most cells in the DEN-induced aggregates were AFP positive, and some of them expressed EpCAM (Figure 4A). However, not all markers were expressed by every cell within a given aggregate, suggesting that the aggregates contain liver cells that are related to bipotential hepatobiliary progenitors/oval cells as well as more differentiated progeny and normal hepatocytes. To confirm these observations, we compared the HcPC and HCC (Figure 3A) to the transcriptome of DDC-induced oval cells (Shin et al., 2011). This analysis revealed a striking similarity between the HCC, HcPC, and the oval cell transcriptomes (Figure S3B). Despite these similarities, some genes that were upregulated in HcPC-containing aggregates and HCC were not upregulated in oval cells. Such genes may account for the tumorigenic properties of HcPC and HCC.

We examined the aggregates for signaling pathways and transcription factors involved in hepatocarcinogenesis. Many aggregated cells were positive for phosphorylated c-Jun and STAT3 (Figure 4A), transcription factors involved in DEN-induced

comparison are highlighted in red, and in the right panel, genes with an FDR < 0.01 in the HCC versus normal comparison are highlighted in cyan. DE, differentially expressed.

(B) Venn diagram showing overlap between genes that are differentially expressed between aggregated and nonaggregated hepatocytes and between HCC cells and normal hepatocytes with an FDR < 0.01 (cyan and red dots from A). The probability to find 583 overlapping genes is $<7.13 \times 10^{-243}$. From these 583 common genes, only 4 behaved differently.

(C) The ten most enriched biological processes (upper table) and cellular compartments (lower panel) represented by genes that are significantly upregulated (left panel) or downregulated (right panel) in HCC relative to normal hepatocytes (HCC) or in aggregated relative to nonaggregated hepatocytes (aggregated).

(D) Heatmap displaying positive fold changes (FC) in expression of genes of interest in aggregated versus nonaggregated HcPCs (left) and in HCC versus normal hepatocytes (right).

(E) Expression of selected genes was examined by real-time PCR and is depicted as fold change relative to normal hepatocytes given an arbitrary value of 1.0 (n = 3; ± SD). (1) Normal hepatocytes; (2) nonaggregated hepatocytes from DEN-treated liver; (3) HcPC aggregates from DEN-treated liver; and (4) DEN-induced HCCs.

See also Figure S3.

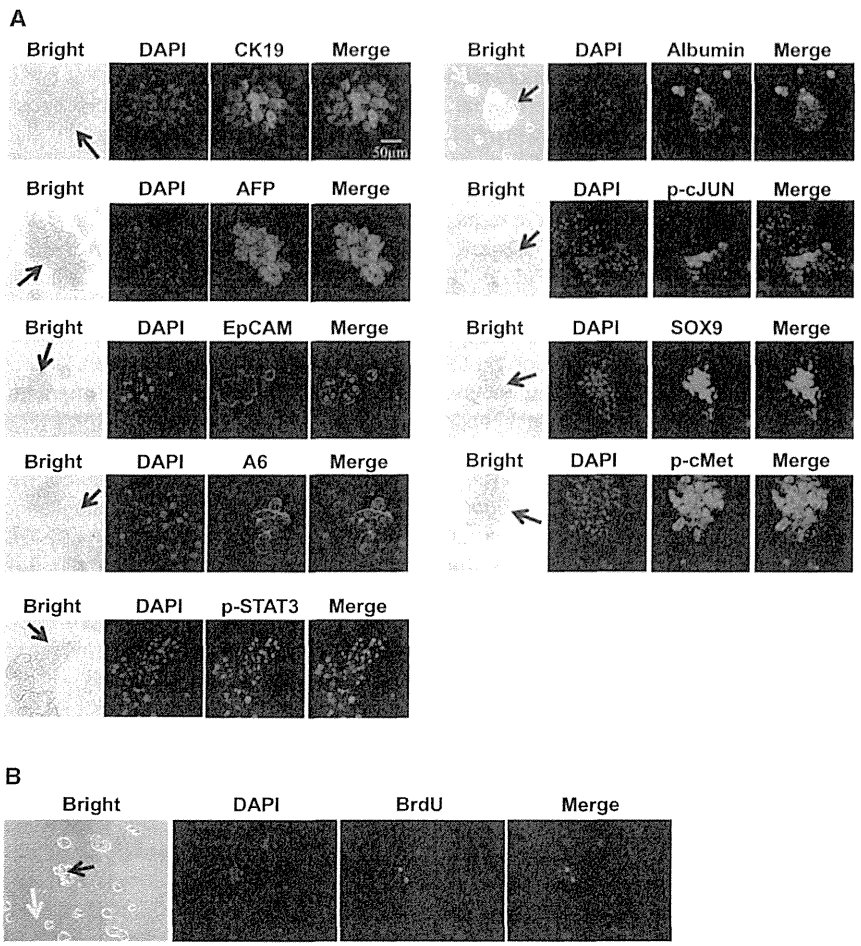

Figure 4. DEN-Induced HcPC Aggregates Express Pathways and Markers Characteristic of HCC and Hepatobiliary Stem Cells

(A) Cytospin preps of collagenase-resistant aggregates from 5-month-old DEN-injected mice were stained with antibodies to CK19, AFP, EpCAM, A6, phospho-Y-STAT3 (Tyr705), albumin, phospho-c-Jun, Sox9, and phospho-c-Met. Black arrows indicate aggregates, and yellow arrows indicate nonaggregated cells (magnification: 400×).

(B) 5-month-old DEN-treated mice were injected with BrdU, and 2 hr later, collagenase-resistant aggregates were isolated and analyzed for BrdU incorporation (400×).

See also Figure S4.

hepatocarcinogenesis (Eferl et al., 2003; He et al., 2010). Sox9, a transcription factor that marks hepatobiliary progenitors (Dorrell et al., 2011), was also expressed by many of the aggregated cells, which were also positive for phosphorylated c-Met (Figure 4A), a receptor tyrosine kinase that is activated by hepatocyte growth factor (HGF) and is essential for liver development (Bladt et al., 1995) and hepatocarcinogenesis (Wang et al., 2001). Few of the nonaggregated hepatocytes exhibited activation of these signaling pathways. Aggregates from bromodeoxyuridine (BrdU)-pulsed DEN-treated mice contained BrdU-positive cells (Figure 4B), indicating that they were actively proliferating prior to isolation. Hepatocyte aggregates from 1-month-old *Tak1*$^{\Delta hep}$ mice also contained cells positive for AFP, Sox9, phosphorylated c-Met, and EpCAM, but not A6-positive cells (Figure S4A). Many of the cells also exhibited partially activated β-catenin, phosphorylated STAT3, and phosphorylated c-Jun. Thus, despite different etiology, HcPC-containing aggregates from *Tak1*$^{\Delta hep}$ mice exhibit upregulation of many of the same markers and pathways that are upregulated in DEN-induced HcPC-containing aggregates. Flow cytometry confirmed enrichment of CD44$^+$ cells as well as CD44$^+$/CD90$^+$ and CD44$^+$/EpCAM$^+$ double-positive cells in the HcPC-containing aggregates from either DEN-treated or *Tak1*$^{\Delta hep}$ livers (Figure S4B).

HcPC-Containing Aggregates Originate from Premalignant Dysplastic Lesions

FAH are dysplastic lesions occurring in rodent livers exposed to hepatic carcinogens (Su et al., 1990). Similar lesions are present in premalignant human livers (Su et al., 1997). Yet, it is still debated whether FAH correspond to premalignant lesions or are a reaction to liver injury that does not lead to cancer (Sell and Leffert, 2008). In DEN-treated males, FAH were detected as early as 3 months after DEN administration (Figure 5A), concomitant with the time at which HcPC-containing aggregates were detected. In females, FAH development was delayed. In both genders, FAH were confined to zone 3 and consisted of tightly packed small hepatocytic cells, some of which were proliferative based on BrdU incorporation (Figure 5B). BrdU$^+$ cells were first detected in DEN-treated males and were confined to FAH and rarely detected in age-matched control mice. FAH contained cells positive for the same progenitor cell markers and activated signaling pathways present in HcPC-containing aggregates, including AFP, CD44, and EpCAM (Figure 5C). FAH also contained cells positive for activated STAT3, c-Jun, and PCNA (Figure 5C). Many cells within FAH exhibited strong upregulation of YAP (Figure 5C), a transcriptional coactivator that is negatively regulated by the Hippo pathway and a liver cancer oncoprotein (Zheng et al., 2011). FAH were also enriched in F4/80$^+$ macrophages (Figure 5C). These results suggest that the HcPC-containing aggregates may be derived from FAH.

HcPCs Exhibit Autocrine IL-6 Expression Necessary for HCC Progression

In situ hybridization (ISH) and immunohistochemistry (IHC) revealed that DEN-induced FAH contained IL-6-expressing cells (Figures 6A, 6B, and S5), and freshly isolated DEN-induced aggregates contained more IL-6 messenger RNA (mRNA) than nonaggregated hepatocytes (Figure 6C). We examined several

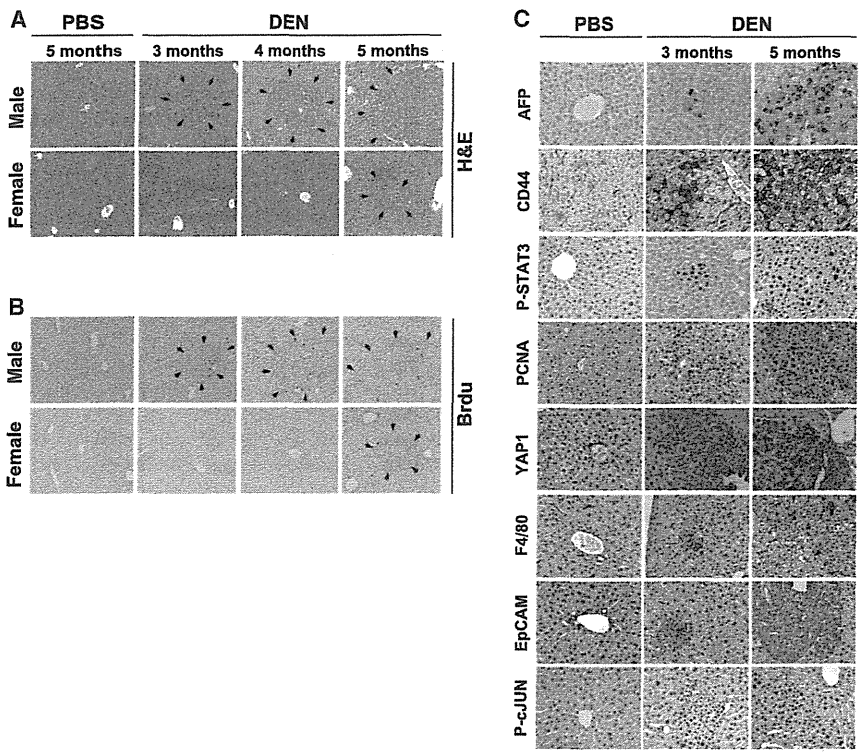

Figure 5. HcPC-Containing Aggregates May Originate from Liver Premalignant Lesions

(A and B) Male and female mice were injected with PBS or DEN at 15 days. At the indicated time points, BrdU was administrated, and livers were collected 2 hr later and stained with H&E (A) or a BrdU-specific antibody (B). Arrows indicate borders of FAH (magnification: 200×).

(C) Sections of male livers treated as above were subjected to IHC with the indicated antibodies (400×).

factors that control IL-6 expression and found that LIN28A and B were significantly upregulated in HcPCs and HCC (Figures 6D and 6E). LIN28-expressing cells were also detected within FAH (Figure 6F). As reported (Iliopoulos et al., 2009), knockdown of LIN28B in cultured HcPC or HCC cell lines decreased IL-6 expression (Figure 6G). LIN28 exerts its effects through downregulation of the microRNA (miRNA) Let-7 (Iliopoulos et al., 2009). Accordingly, miRNA array analysis of aggregated and nonaggregated hepatocytes from DEN-treated mice indicated that the amount of Let-7, along with other miRNAs that also inhibit IL-6 expression (miR194 and miR872), was lower in aggregated cells than in nonaggregated cells (Table S2).

To determine whether autocrine IL-6 production is needed for HCC growth, we silenced IL-6 expression with small hairpin RNA (shRNA) in dih10 HCC cells (He et al., 2010). This resulted in nearly a 75% decrease in IL-6 mRNA (Figure 7A) but had little effect on cell growth in the presence of growth factors, including EGF and insulin (Figure S6A). IL-6 mRNA silencing, however, diminished the ability of dih10 cells to form s.c. tumors (Figures S6B and S6C) and inhibited their ability to form HCCs and proliferate after transplantation into MUP-uPA mice (Figures 7B and S6D). To investigate the importance of autocrine IL-6 production at an earlier step, we isolated HcPC from DEN-treated WT and *Il6*$^{-/-}$ mice. Although IL-6 ablation attenuates HCC induction (Naugler et al., 2007), we still could isolate collagenase-resistant aggregates from livers of DEN-injected *Il6*$^{-/-}$ mice. Notably, IL-6 ablation did not reduce the proportion of CD44^{+} cells in the aggregates (Figures S7A and S7B). We introduced an identical number of WT and *Il6*$^{-/-}$ aggregated hepatocytes into MUP-uPA mice and scored HCC development 5 months later. The IL-6 deficiency resulted in a 2.5-fold decrease in tumorigenic potential (Figure 7C), suggesting that autocrine IL-6 contributes to HcPC to HCC progression. To confirm this point, we dispersed freshly isolated DEN-induced aggregates and transduced them with bicistronic lentiviruses encoding either scrambled or IL-6-specific shRNAs and a GFP marker. After a few days in culture, the transduced cells were introduced into MUP-uPA mice that were examined for HCC development 6 months later. Silencing of IL-6 reduced HCC generation (Figure 7D) and inhibited formation of GFP^{+} colonies within the MUP-uPA liver (Figure 7E). We also ablated IL-6 expression in mouse hepatocytes and found that this led to a marked reduction in DEN-induced tumorigenesis (Figure 7F). Thus, autocrine IL-6 production by DEN-initiated HcPC is important for HCC development. To investigate whether autocrine IL-6 signaling also occurs in human premalignant lesions, we examined needle biopsies of normal liver tissue and HCV-infected livers with dysplastic lesions. We found that 16% of all (n = 25) dysplastic lesions exhibited coexpression of LIN28 and IL-6 and contained activated STAT3 (Figure 7G). These markers were hardly detected in normal liver or nontumor portion of HCV-infected livers.

DISCUSSION

The isolation and characterization of cells that can give rise to HCC only after transplantation into an appropriate host liver undergoing chronic injury demonstrates that cancer arises from progenitor cells that are yet to become fully malignant. Importantly, unlike fully malignant HCC cells, the HcPCs we isolated cannot form s.c. tumors or even liver tumors when introduced into a nondamaged liver. Liver damage induced by uPA expression or CCl_4 treatment provides HcPCs with the proper cytokine and growth factor milieu needed for their proliferation. Although HcPCs produce IL-6, they may also depend on other cytokines such as TNF, which is produced by macrophages that are recruited to the damaged liver. In addition, uPA expression and CCl_4 treatment may enhance HcPC growth and progression through their fibrogenic effect on hepatic stellate cells. Although HCC and other cancers have been suspected to arise from

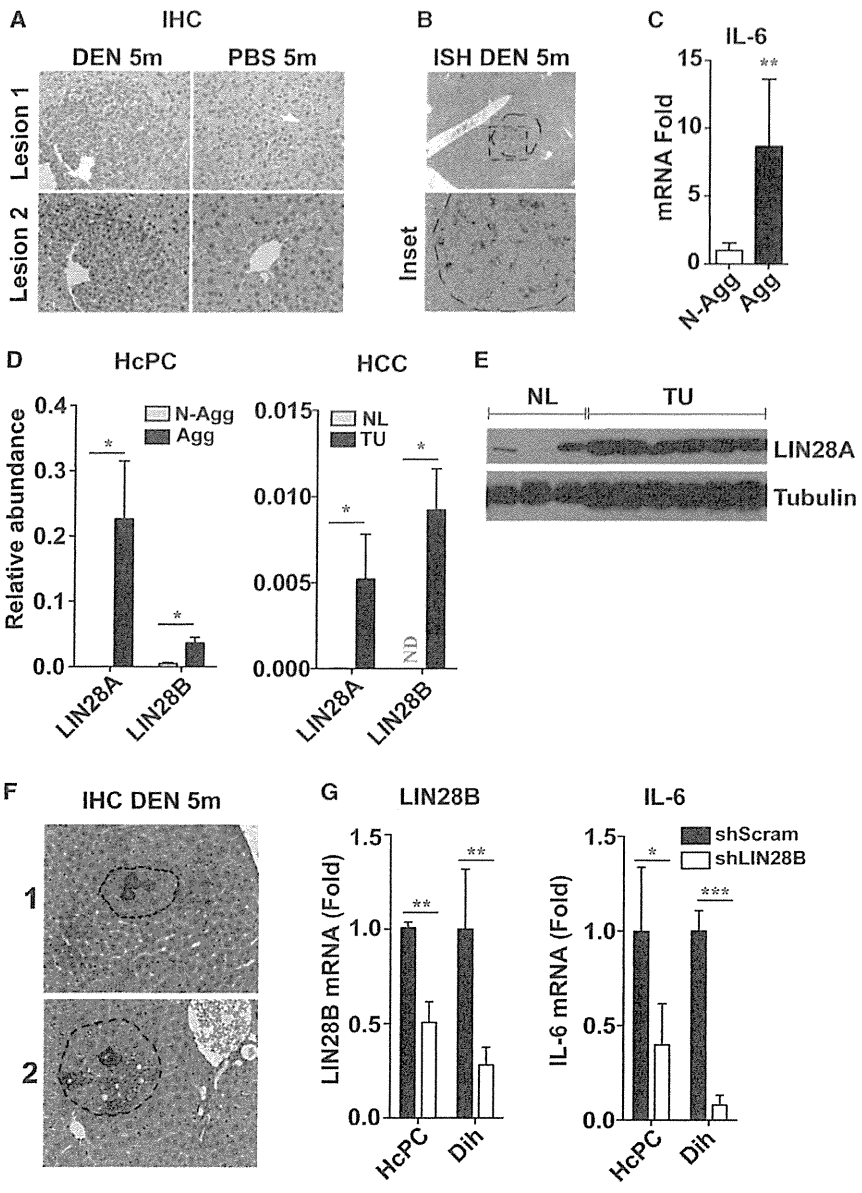

Figure 6. Liver Premalignant Lesions and HcPCs Exhibit Elevated IL-6 and LIN28 Expression

(A and B) Livers of 5-month-old DEN injected mice were analyzed for IL-6 expression by IHC (magnification: 400×) (A) and ISH (magnification: 100×, top; 400×, bottom) (B).

(C and D) Quantification of IL-6 (C) and LIN28 (D) mRNA in aggregated versus nonaggregated hepatocytes from 5-month-old DEN-treated livers and in normal versus tumor-bearing livers (n = 6; ± SEM) (ND, not detected).

(E) Immunoblot analyses of LIN28A in normal (NL) and tumor-bearing (TU) livers.

(F) DEN-treated livers were subjected to IHC with a LIN28A antibody. Broken lines indicate borders of FAH (400×).

(G) LIN28B was silenced with shRNA in HCC (dih) cells and cultured HcPCs, and LIN28B and IL-6 mRNAs were quantitated by qRT-PCR (n = 3; ± SEM).

See also Figure S5 and Table S2.

premalignant/dysplastic lesions (Hruban et al., 2007; Hytiroglou et al., 2007), a direct demonstration that such lesions progress into malignant tumors has been lacking. Based on expression of common markers—EpCAM, CD44, AFP, activated STAT3, and IL-6—that are not expressed in normal hepatocytes, we postulate that HcPCs originate from FAH or dysplastic foci, which are first observed in male mice within 3 months of DEN exposure. Indeed, the cells that are contained within the FAH are smaller than the surrounding parenchyma and are similar in size to isolated HcPCs. Importantly, FAH or premalignant dysplastic foci are not unique to DEN-treated rodents (Bannasch, 1984; Rabes, 1983), and similar lesions were detected in human cirrhotic livers (Hytiroglou et al., 2007; Seki et al., 2000; Takayama et al., 1990) in which the rate of HCC progression is 3%–5% per year (El-Serag, 2011). We found that human dysplastic lesions and mouse FAH and HcPC exhibit autocrine IL-6 signaling. HcPC are not unique to DEN-treated mice, and similar cells were isolated from *Tak1*$^{\Delta hep}$ mice in which HCC development resembles cirrhosis-associated human HCC (Inokuchi et al., 2010).

HcPC Origin and Relationship to Liver and HCC Stem Cells

Transcriptomic analysis indicates that DEN-induced HcPCs are related to both normal hepatobiliary bipotential stem cells/oval cells and HCC cells. Although HcPCs are not fully transformed, they express several markers—CD44, EpCAM, AFP, SOX9, OV6, and CK19—found to be expressed by HCC stem cells and oval cells (Guo et al., 2012; Mikhail and He, 2011; Terris et al., 2010; Yamashita et al., 2008; Zhu et al., 2010). However, unlike oval cells, which do not express albumin or AFP and do not give rise to liver tumors upon transplantation into MUP-uPA mice, HcPCs give rise to HCC after intrasplenic transplantation. Yet, unlike dih10 HCC cells, which express high levels of the HCC stem cell markers AFP, CD44, and EpCAM, HcPCs do not form s.c. tumors.

At this point, it is not clear whether HcPCs arise from oval cells or from dedifferentiated hepatocytes. Given that DEN is metabolically activated by Cyp2E1 that is expressed only in fully differentiated zone 3 hepatocytes (Tsutsumi et al., 1989) and that *Cyp2E1*$^{-/-}$ mice are refractory to DEN (Kang et al., 2007), DEN-induced HcPC are most likely derived from dedifferentiated hepatocytes. Consistent with this hypothesis, DEN-induced FAH and proliferating cells were found in zone 3 and not near bile ducts or the canals of Hering, sites at which oval cells reside

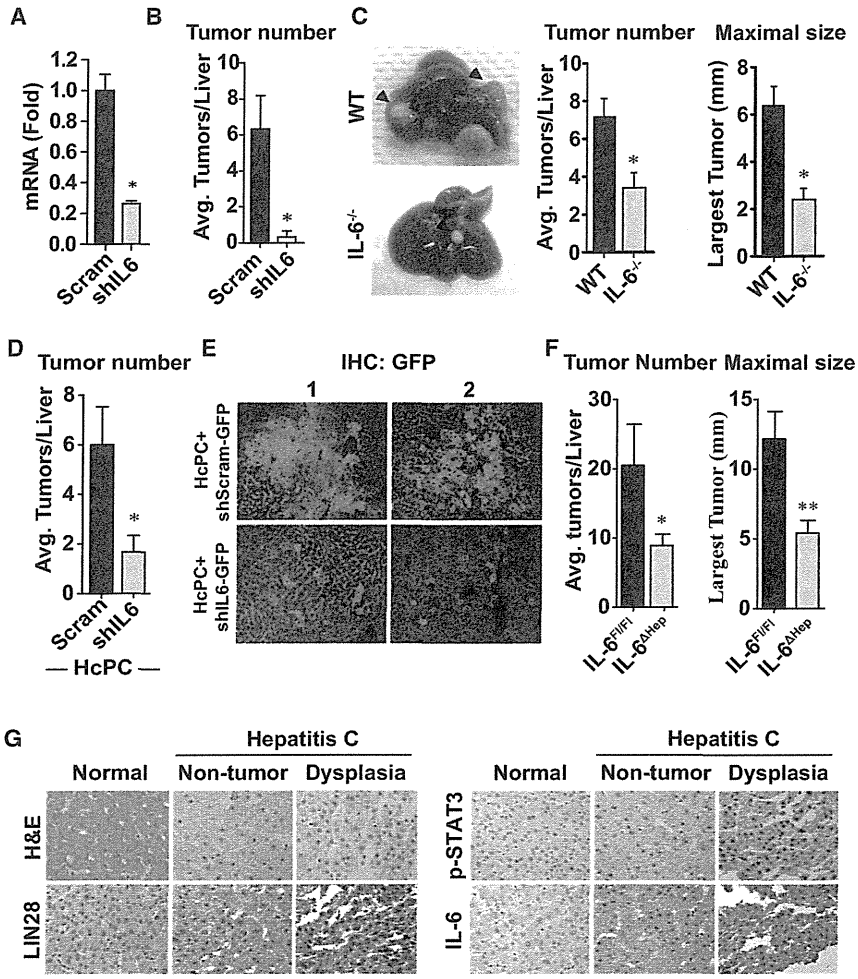

Figure 7. HCC Growth Depends on Autocrine IL-6 Production

(A) HCC cells (dih10) were transduced with lentiviruses containing scrambled or IL-6-specific shRNA. IL-6 mRNA was analyzed by qRT-PCR.

(B) Dih10 cells (1.2×10^5) transduced as above were i.s. injected into MUP-uPA mice that were analyzed 6 months later for HCC development (n = 3; ± SEM).

(C) HcPCs from WT and *Il6*$^{-/-}$ mice were injected (1×10^4 cells/mice) into MUP-uPA mice and analyzed 5 months later for HCC development (n = 5; ± SEM).

(D) HcPCs isolated from DEN-treated WT mice were transduced with shRNA against IL-6 or scrambled shRNA, cultured for 3 to 4 days, i.s. transplanted (1×10^4 cells/mice) into MUP-uPA mice, and analyzed 6 months later (n = 3; ± SEM).

(E) Livers of MUP-uPA mice from (D) were immunostained with GFP antibody 6 months after transplantation (200×). The bicistronic lentivirus in this experiment expresses GFP along with control or IL-6 shRNA, allowing tracking of the infected cells.

(F) DEN-treated *Il6*$^{\Delta hep}$ and *Il6*$^{F/F}$ mice were sacrificed after 9 months to evaluate tumor multiplicity and size (n = 6–10, ± SEM).

(G) IHC analysis of autocrine IL-6 signaling in human premalignant lesions in HCV-infected livers. Expression of LIN28, p-STAT3, and IL-6 was analyzed in 25 needle biopsies of dysplastic nodules, and representative positive specimens (n = 4) are shown. The dysplastic nodules and paired nontumor tissue were obtained from the same HCV-infected patient (n = 25). Nontumor tissue of metastatic liver cancer was used as normal control.

See also Figures S6 and S7.

(Duncan et al., 2009). Notably, GO analysis revealed that many of the genes whose expression is downregulated in HcPC-containing aggregates are involved in xenobiotic and organic acid metabolism, characteristics of differentiated hepatocytes. The same types of genes are also downregulated in HCC. However, final identification of the origin of HcPC will be provided by ongoing lineage-tracing experiments.

The Significance of Autocrine IL-6 Expression

Elevated IL-6 was detected in at least 40% of human HCCs, where it is expressed by the cancer cells (Soresi et al., 2006). More recent studies have confirmed upregulation of IL-6 in human HCC and suggested that it plays a central role in a gene expression network that drives tumor development (Ji et al., 2009). Elevated IL-6 was also found in viral and alcoholic hepatitis and liver cirrhosis, but in these conditions, IL-6 is expressed mainly by myeloid cells/leukocytes rather than parenchymal cells (Deviere et al., 1989; Kakumu et al., 1993; Soresi et al., 2006). Our studies indicate that the critical site of IL-6 expression shifts from myeloid cells to epithelial cells during the course of DEN-induced liver tumorigenesis. Initially, DEN administration rapidly induces IL-6 in Kupffer cells through NF-κB activation (Maeda et al., 2005). This initial surge in IL-6 is required for DEN-induced hepatocarcinogenesis (Naugler et al., 2007). Although IL-6 decays within 2 weeks of DEN administration, it reappears several months later, but at that time, it is expressed within FAH. IL-6 expression is also elevated in isolated HcPCs and is maintained in fully transformed HCC cells. Furthermore, autocrine IL-6 is important for HcPC to HCC progression and for tumorigenic growth. Autocrine IL-6 in both HcPC and HCC cells depends on elevated expression of LIN28, an RNA-binding protein that exerts its protumorigenic activity through downregulation of Let-7, an miRNA that inhibits IL-6 expression (Viswanathan and Daley, 2010). Accordingly, HcPCs exhibit downregulation of both Let-7f and Let-7g, and elevated LIN28 is found not only in isolated HcPCs but also within FAH and human HCV-induced dysplastic lesions.

A similar LIN28-Let-7-IL-6 epigenetic switch is important for in vitro programming and maintenance of cancer stem cells (Iliopoulos et al., 2009). IL-6 also induces malignant features in human ductal carcinoma stem cells (Sansone et al., 2007). In fact, autocrine IL-6 signaling was suggested to play a key role in STAT3-dependent tumor progression (Grivennikov and Karin, 2008). Another miRNA-driven autoregulatory circuit involved in

hepatocarcinogenesis accounts for elevated IL-6R expression (Hatziapostolou et al., 2011). Yet, HcPC-containing aggregates also express several other STAT3-activiting cytokines and receptors. Accordingly, silencing or ablation of IL-6 results in incomplete inhibition of HcPC to HCC progression. Nonetheless, our results demonstrate that autoregulatory circuits/epigenetic switches play an important role in the very early stages of tumorigenesis. Given that such circuits are already activated in premalignant cells, pharmacological agents that disrupt their function may be useful in cancer prevention. Prevention is of particular importance in cancers such as HCC, which is often detected at a stage that is refractory to currently available therapeutics.

EXPERIMENTAL PROCEDURES

Mice, HCC Induction, HcPC Isolation, and Transplantation

MUP-uPA transgenic mice (Weglarz et al., 2000) were maintained on a pure BL/6 background. Because homozygous females frequently die when pregnant, MUP-uPA heterozygotes were generated by backcrossing homozygous MUP-uPA males with BL/6 females to be used as recipients for hepatic transplantation. *Tak1*$^{\Delta hep}$ (Inokuchi et al., 2010) and *Il6*$^{F/F}$ (Quintana et al., 2013) mice were also in the BL/6 background. *Il6*$^{\Delta hep}$ mice were generated by crossing *Il6*$^{F/F}$ and *Alb-Cre* mice. C57BL/6 actin-GFP mice were from the Jackson Laboratories. BL/6 mice were purchased from Charles River Laboratories.

To induce HCC, 15-day-old mice were injected i.p. with 25 mg/kg DEN (Sigma). A pool of DEN-injected BL/6 mice was maintained and used in most experiments. Hepatocytes were isolated using a two-step procedure (He et al., 2010). Cell aggregates were isolated by filtration through 70 and 40 μm sieves. To disperse the aggregates into single cells, they were subjected to gentle pipetting in Ca/Mg-free PBS on ice. Single-cell suspensions of aggregated and nonaggregated hepatocytes were transplanted via an i.s. injection into 21-day-old male MUP-uPA mice (He et al., 2010). Alternatively, single-cell suspensions of aggregated hepatocytes were enriched for CD44^{+} HcPC using magnetic beads. As few as 100 viable CD44^{+} cells mixed with 1 × 10^{5} normal hepatocytes from normal males were transplanted into MUP-uPA mice. Alternatively, BL/6 mice were pretreated with retrorsine (70 mg/kg i.p.) (Sigma), a cell-cycle inhibitor, 1 month prior to transplantation. Transplanted mice were allowed to recover for 1 week and then injected weekly with 3× 0.5 ml/kg CCl_4 i.p. to induce liver injury and hepatocyte proliferation (Guo et al., 2002). Mice were sacrificed 5 to 6 months later, and tumors bigger than 1 mm in diameter on the liver surface were counted. Tumors bigger than 5 mm across were dissected for biochemical and molecular analyses.

ACCESSION NUMBERS

Raw gene expression array data have been deposited to NCBI's Gene Expression Omnibus under the GSE50431 study.

SUPPLEMENTAL INFORMATION

Supplemental Information includes Extended Experimental Procedures, seven figures, and three tables and can be found with this article online at http://dx.doi.org/10.1016/j.cell.2013.09.031.

AUTHOR CONTRIBUTIONS

G.H. identified, isolated, and characterized HcPCs; D.D. and H.N. optimized the HcPC isolation and purification procedure; D.D. found the mechanism of their dependence on autocrine IL-6 controlled by LIN28, characterized them using flow cytometry (with S.S.), and conducted miR analyses (with M.H. and D.I.); H.N. and D.D. used *Il6*$^{\Delta hep}$ mice to demonstrate in vivo HCC dependency on autocrine IL-6; H.N. (with R.T. and K.K.) found IL-6, LIN28, and P-STAT3 in human dysplastic lesions; J.F.-B. conducted the transcriptome analysis and exome sequencing (with S.E.Y., K.J., and O.H.) and with H.O. examined oncogenic potential of oval cells; H.O. examined HcPC proliferative potential and performed IF analysis of isolated HcPC (with A.S. and R.M.H.); Y.J. assisted with IHC and ISH staining; E.S. contributed to the experiments involving *Tak1*$^{\Delta hep}$ mice; G.H., D.D., J.F.-B., H.O., and M.K. wrote the manuscript.

ACKNOWLEDGMENTS

We acknowledge the Biogem facility at UCSD for their assistance with transcriptome analysis and A. Arian, K. Iwaisako, Y. Hiroshima, and H. Matsui for technical assistance. We thank Dr. J. Hidalgo (Universitat Autonoma de Barcelona, Spain) for the *Il6*$^{F/F}$ mice. Research was supported by the Superfund Basic Research Program (P42ES010337), NIH (CA118165 and CA155120), Wellcome Trust (WT086755), American Diabetes Association (7-08-MN-29), the Center for Translational Science (UL1RR031980 and UL1TR000100), the National Center for Research Resources IMAT program (N12R1CA155615), and postdoctoral research fellowships from the Damon Runyon Cancer Research Foundation (G.H.), American Liver Foundation (D.D.), Daiichi Sankyo Foundation of Life Science (H.N.), California Institute for Regenerative Medicine Stem Cell Training Grant II (TG2-01154) fellowship (J.F.-B.), Kanzawa Medical Research Foundation (H.O.), the German Research Foundation (DFG, SH721/1-1 to S.S.), and a Young Investigator Award from the National Childhood Cancer Foundation, "CureSearch" (D.D.). M.K. is an ACS Research Professor and is a recipient of the Ben and Wanda Hildyard Chair for Mitochondrial and Metabolic Diseases.

Received: December 11, 2012
Revised: June 4, 2013
Accepted: September 19, 2013
Published: October 10, 2013

REFERENCES

Bannasch, P. (1984). Sequential cellular changes during chemical carcinogenesis. J. Cancer Res. Clin. Oncol. *108*, 11–22.

Bladt, F., Riethmacher, D., Isenmann, S., Aguzzi, A., and Birchmeier, C. (1995). Essential role for the c-met receptor in the migration of myogenic precursor cells into the limb bud. Nature *376*, 768–771.

Deviere, J., Content, J., Denys, C., Vandenbussche, P., Schandene, L., Wybran, J., and Dupont, E. (1989). High interleukin-6 serum levels and increased production by leucocytes in alcoholic liver cirrhosis. Correlation with IgA serum levels and lymphokines production. Clin. Exp. Immunol. *77*, 221–225.

Dorrell, C., Erker, L., Schug, J., Kopp, J.L., Canaday, P.S., Fox, A.J., Smirnova, O., Duncan, A.W., Finegold, M.J., Sander, M., et al. (2011). Prospective isolation of a bipotential clonogenic liver progenitor cell in adult mice. Genes Dev. *25*, 1193–1203.

Duncan, A.W., Dorrell, C., and Grompe, M. (2009). Stem cells and liver regeneration. Gastroenterology *137*, 466–481.

Eferl, R., Ricci, R., Kenner, L., Zenz, R., David, J.P., Rath, M., and Wagner, E.F. (2003). Liver tumor development. c-Jun antagonizes the proapoptotic activity of p53. Cell *112*, 181–192.

El-Serag, H.B. (2011). Hepatocellular carcinoma. N. Engl. J. Med. *365*, 1118–1127.

Grivennikov, S., and Karin, M. (2008). Autocrine IL-6 signaling: a key event in tumorigenesis? Cancer Cell *13*, 7–9.

Guichard, C., Amaddeo, G., Imbeaud, S., Ladeiro, Y., Pelletier, L., Maad, I.B., Calderaro, J., Bioulac-Sage, P., Letexier, M., Degos, F., et al. (2012). Integrated analysis of somatic mutations and focal copy-number changes identifies key genes and pathways in hepatocellular carcinoma. Nat. Genet. *44*, 694–698.

Guo, D., Fu, T., Nelson, J.A., Superina, R.A., and Soriano, H.E. (2002). Liver repopulation after cell transplantation in mice treated with retrorsine and carbon tetrachloride. Transplantation *73*, 1818–1824.

Guo, X., Xiong, L., Sun, T., Peng, R., Zou, L., Zhu, H., Zhang, J., Li, H., and Zhao, J. (2012). Expression features of SOX9 associate with tumor progression and poor prognosis of hepatocellular carcinoma. Diagn. Pathol. *7*, 44.

Haridass, D., Yuan, Q., Becker, P.D., Cantz, T., Iken, M., Rothe, M., Narain, N., Bock, M., Nörder, M., Legrand, N., et al. (2009). Repopulation efficiencies of adult hepatocytes, fetal liver progenitor cells, and embryonic stem cell-derived hepatic cells in albumin-promoter-enhancer urokinase-type plasminogen activator mice. Am. J. Pathol. *175*, 1483–1492.

Hatziapostolou, M., Polytarchou, C., Aggelidou, E., Drakaki, A., Poultsides, G.A., Jaeger, S.A., Ogata, H., Karin, M., Struhl, K., Hadzopoulou-Cladaras, M., and Iliopoulos, D. (2011). An HNF4α-miRNA inflammatory feedback circuit regulates hepatocellular oncogenesis. Cell *147*, 1233–1247.

He, G., Yu, G.Y., Temkin, V., Ogata, H., Kuntzen, C., Sakurai, T., Sieghart, W., Peck-Radosavljevic, M., Leffert, H.L., and Karin, M. (2010). Hepatocyte IKKbeta/NF-kappaB inhibits tumor promotion and progression by preventing oxidative stress-driven STAT3 activation. Cancer Cell *17*, 286–297.

Hruban, R.H., Maitra, A., Kern, S.E., and Goggins, M. (2007). Precursors to pancreatic cancer. Gastroenterol. Clin. North Am. *36*, 831–849, vi.

Hytiroglou, P., Park, Y.N., Krinsky, G., and Theise, N.D. (2007). Hepatic precancerous lesions and small hepatocellular carcinoma. Gastroenterol. Clin. North Am. *36*, 867–887, vii.

Ichinohe, N., Kon, J., Sasaki, K., Nakamura, Y., Ooe, H., Tanimizu, N., and Mitaka, T. (2012). Growth ability and repopulation efficiency of transplanted hepatic stem cells, progenitor cells, and mature hepatocytes in retrorsine-treated rat livers. Cell Transplant. *21*, 11–22.

Iliopoulos, D., Hirsch, H.A., and Struhl, K. (2009). An epigenetic switch involving NF-kappaB, Lin28, Let-7 MicroRNA, and IL6 links inflammation to cell transformation. Cell *139*, 693–706.

Inokuchi, S., Aoyama, T., Miura, K., Osterreicher, C.H., Kodama, Y., Miyai, K., Akira, S., Brenner, D.A., and Seki, E. (2010). Disruption of TAK1 in hepatocytes causes hepatic injury, inflammation, fibrosis, and carcinogenesis. Proc. Natl. Acad. Sci. USA *107*, 844–849.

Ji, J., Shi, J., Budhu, A., Yu, Z., Forgues, M., Roessler, S., Ambs, S., Chen, Y., Meltzer, P.S., Croce, C.M., et al. (2009). MicroRNA expression, survival, and response to interferon in liver cancer. N. Engl. J. Med. *361*, 1437–1447.

Kakumu, S., Shinagawa, T., Ishikawa, T., Yoshioka, K., Wakita, T., and Ida, N. (1993). Interleukin 6 production by peripheral blood mononuclear cells in patients with chronic hepatitis B virus infection and primary biliary cirrhosis. Gastroenterol. Jpn. *28*, 18–24.

Kang, J.S., Wanibuchi, H., Morimura, K., Gonzalez, F.J., and Fukushima, S. (2007). Role of CYP2E1 in diethylnitrosamine-induced hepatocarcinogenesis in vivo. Cancer Res. *67*, 11141–11146.

Laconi, E., Oren, R., Mukhopadhyay, D.K., Hurston, E., Laconi, S., Pani, P., Dabeva, M.D., and Shafritz, D.A. (1998). Long-term, near-total liver replacement by transplantation of isolated hepatocytes in rats treated with retrorsine. Am. J. Pathol. *153*, 319–329.

Maeda, S., Kamata, H., Luo, J.L., Leffert, H., and Karin, M. (2005). IKKbeta couples hepatocyte death to cytokine-driven compensatory proliferation that promotes chemical hepatocarcinogenesis. Cell *121*, 977–990.

Marquardt, J.U., and Thorgeirsson, S.S. (2010). Stem cells in hepatocarcinogenesis: evidence from genomic data. Semin. Liver Dis. *30*, 26–34.

Meyer, K., Lee, J.S., Dyck, P.A., Cao, W.Q., Rao, M.S., Thorgeirsson, S.S., and Reddy, J.K. (2003). Molecular profiling of hepatocellular carcinomas developing spontaneously in acyl-CoA oxidase deficient mice: comparison with liver tumors induced in wild-type mice by a peroxisome proliferator and a genotoxic carcinogen. Carcinogenesis *24*, 975–984.

Mikhail, S., and He, A.R. (2011). Liver cancer stem cells. Int. J. Hepatol. *2011*, 486954.

Naugler, W.E., Sakurai, T., Kim, S., Maeda, S., Kim, K., Elsharkawy, A.M., and Karin, M. (2007). Gender disparity in liver cancer due to sex differences in MyD88-dependent IL-6 production. Science *317*, 121–124.

Nguyen, L.V., Vanner, R., Dirks, P., and Eaves, C.J. (2012). Cancer stem cells: an evolving concept. Nat. Rev. Cancer *12*, 133–143.

Nowell, P.C. (1976). The clonal evolution of tumor cell populations. Science *194*, 23–28.

Park, E.J., Lee, J.H., Yu, G.Y., He, G., Ali, S.R., Holzer, R.G., Osterreicher, C.H., Takahashi, H., and Karin, M. (2010). Dietary and genetic obesity promote liver inflammation and tumorigenesis by enhancing IL-6 and TNF expression. Cell *140*, 197–208.

Pitot, H.C. (1990). Altered hepatic foci: their role in murine hepatocarcinogenesis. Annu. Rev. Pharmacol. Toxicol. *30*, 465–500.

Porta, C., De Amici, M., Quaglini, S., Paglino, C., Tagliani, F., Boncimino, A., Moratti, R., and Corazza, G.R. (2008). Circulating interleukin-6 as a tumor marker for hepatocellular carcinoma. Ann. Oncol. *19*, 353–358.

Quintana, A., Erta, M., Ferrer, B., Comes, G., Giralt, M., and Hidalgo, J. (2013). Astrocyte-specific deficiency of interleukin-6 and its receptor reveal specific roles in survival, body weight and behavior. Brain Behav. Immun. *27*, 162–173.

Rabes, H.M. (1983). Development and growth of early preneoplastic lesions induced in the liver by chemical carcinogens. J. Cancer Res. Clin. Oncol. *106*, 85–92.

Rhim, J.A., Sandgren, E.P., Degen, J.L., Palmiter, R.D., and Brinster, R.L. (1994). Replacement of diseased mouse liver by hepatic cell transplantation. Science *263*, 1149–1152.

Sansone, P., Storci, G., Tavolari, S., Guarnieri, T., Giovannini, C., Taffurelli, M., Ceccarelli, C., Santini, D., Paterini, P., Marcu, K.B., et al. (2007). IL-6 triggers malignant features in mammospheres from human ductal breast carcinoma and normal mammary gland. J. Clin. Invest. *117*, 3988–4002.

Seki, S., Sakaguchi, H., Kitada, T., Tamori, A., Takeda, T., Kawada, N., Habu, D., Nakatani, K., Nishiguchi, S., and Shiomi, S. (2000). Outcomes of dysplastic nodules in human cirrhotic liver: a clinicopathological study. Clin. Cancer Res. *6*, 3469–3473.

Sell, S., and Leffert, H.L. (2008). Liver cancer stem cells. J. Clin. Oncol. *26*, 2800–2805.

Shin, S., Walton, G., Aoki, R., Brondell, K., Schug, J., Fox, A., Smirnova, O., Dorrell, C., Erker, L., Chu, A.S., et al. (2011). Foxl1-Cre-marked adult hepatic progenitors have clonogenic and bilineage differentiation potential. Genes Dev. *25*, 1185–1192.

Soresi, M., Giannitrapani, L., D'Antona, F., Florena, A.M., La Spada, E., Terranova, A., Cervello, M., D'Alessandro, N., and Montalto, G. (2006). Interleukin-6 and its soluble receptor in patients with liver cirrhosis and hepatocellular carcinoma. World J. Gastroenterol. *12*, 2563–2568.

Su, Y., Kanamoto, R., Miller, D.A., Ogawa, H., and Pitot, H.C. (1990). Regulation of the expression of the serine dehydratase gene in the kidney and liver of the rat. Biochem. Biophys. Res. Commun. *170*, 892–899.

Su, Q., Benner, A., Hofmann, W.J., Otto, G., Pichlmayr, R., and Bannasch, P. (1997). Human hepatic preneoplasia: phenotypes and proliferation kinetics of foci and nodules of altered hepatocytes and their relationship to liver cell dysplasia. Virchows Arch. *431*, 391–406.

Takayama, T., Makuuchi, M., Hirohashi, S., Sakamoto, M., Okazaki, N., Takayasu, K., Kosuge, T., Motoo, Y., Yamazaki, S., and Hasegawa, H. (1990). Malignant transformation of adenomatous hyperplasia to hepatocellular carcinoma. Lancet *336*, 1150–1153.

Terris, B., Cavard, C., and Perret, C. (2010). EpCAM, a new marker for cancer stem cells in hepatocellular carcinoma. J. Hepatol. *52*, 280–281.

Tsutsumi, M., Lasker, J.M., Shimizu, M., Rosman, A.S., and Lieber, C.S. (1989). The intralobular distribution of ethanol-inducible P450IIE1 in rat and human liver. Hepatology *10*, 437–446.

Verna, L., Whysner, J., and Williams, G.M. (1996). N-nitrosodiethylamine mechanistic data and risk assessment: bioactivation, DNA-adduct formation, mutagenicity, and tumor initiation. Pharmacol. Ther. *71*, 57–81.

Viswanathan, S.R., and Daley, G.Q. (2010). Lin28: A microRNA regulator with a macro role. Cell *140*, 445–449.

Wang, R., Ferrell, L.D., Faouzi, S., Maher, J.J., and Bishop, J.M. (2001). Activation of the Met receptor by cell attachment induces and sustains hepatocellular carcinomas in transgenic mice. J. Cell Biol. *153*, 1023–1034.

Weglarz, T.C., Degen, J.L., and Sandgren, E.P. (2000). Hepatocyte transplantation into diseased mouse liver. Kinetics of parenchymal repopulation and identification of the proliferative capacity of tetraploid and octaploid hepatocytes. Am. J. Pathol. *157*, 1963–1974.

Wood, L.D., Parsons, D.W., Jones, S., Lin, J., Sjöblom, T., Leary, R.J., Shen, D., Boca, S.M., Barber, T., Ptak, J., et al. (2007). The genomic landscapes of human breast and colorectal cancers. Science *318*, 1108–1113.

Yamashita, T., Forgues, M., Wang, W., Kim, J.W., Ye, Q., Jia, H., Budhu, A., Zanetti, K.A., Chen, Y., Qin, L.X., et al. (2008). EpCAM and alpha-fetoprotein expression defines novel prognostic subtypes of hepatocellular carcinoma. Cancer Res. *68*, 1451–1461.

Yang, Z.F., Ho, D.W., Ng, M.N., Lau, C.K., Yu, W.C., Ngai, P., Chu, P.W., Lam, C.T., Poon, R.T., and Fan, S.T. (2008). Significance of CD90+ cancer stem cells in human liver cancer. Cancer Cell *13*, 153–166.

Zheng, T., Wang, J., Jiang, H., and Liu, L. (2011). Hippo signaling in oval cells and hepatocarcinogenesis. Cancer Lett. *28*, 91–99.

Zhu, Z., Hao, X., Yan, M., Yao, M., Ge, C., Gu, J., and Li, J. (2010). Cancer stem/progenitor cells are highly enriched in CD133+CD44+ population in hepatocellular carcinoma. Int. J. Cancer *126*, 2067–2078.

Zöller, M. (2009). Tetraspanins: push and pull in suppressing and promoting metastasis. Nat. Rev. Cancer *9*, 40–55.

SCIENTIFIC REPORTS

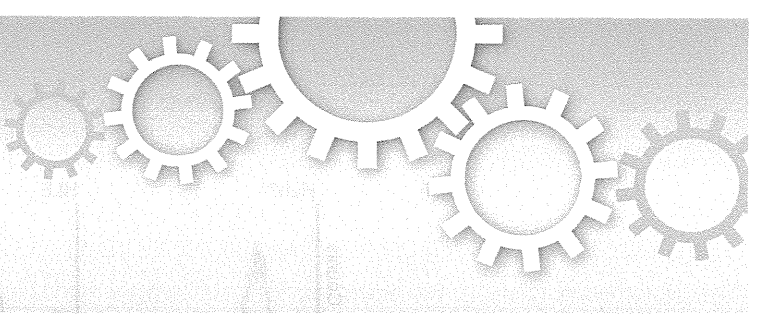

OPEN

SUBJECT AREAS:
TUMOUR IMMUNOLOGY
CANCER PREVENTION
LIVER CANCER
TRANSLATIONAL RESEARCH

Received
2 May 2013

Accepted
4 September 2013

Published
24 September 2013

Correspondence and requests for materials should be addressed to M.O. (otsukamo-tky@umin.ac.jp)

*These authors contributed equally to this work.

Regulation of the expression of the liver cancer susceptibility gene MICA by microRNAs

Takahiro Kishikawa[1]*, Motoyuki Otsuka[1,2]*, Takeshi Yoshikawa[1], Motoko Ohno[1], Akemi Takata[1], Chikako Shibata[1], Yuji Kondo[1], Masao Akanuma[3], Haruhiko Yoshida[1] & Kazuhiko Koike[1]

[1]Department of Gastroenterology, Graduate School of Medicine, The University of Tokyo, Tokyo 113-8655, Japan, [2]Japan Science and Technology Agency, PRESTO, Kawaguchi, Saitama 332-0012, Japan, [3]Division of Gastroenterology, The Institute for Adult Diseases, Asahi Life Foundation, Tokyo 100-0005, Japan.

Hepatocellular carcinoma (HCC) is a threat to public health worldwide. We previously identified the association of a single nucleotide polymorphism (SNP) at the promoter region of the MHC class I polypeptide-related sequence A (MICA) gene with the risk of hepatitis-virus-related HCC. Because this SNP affects MICA expression levels, regulating MICA expression levels may be important in the prevention of HCC. We herein show that the microRNA (miR) 25-93-106b cluster can modulate MICA levels in HCC cells. Overexpression of the miR 25-93-106b cluster significantly suppressed MICA expression. Conversely, silencing of this miR cluster enhanced MICA expression in cells that express substantial amounts of MICA. The changes in MICA expression levels by the miR25-93-106b cluster were biologically significant in an NKG2D-binding assay and an *in vivo* cell-killing model. These data suggest that the modulation of MICA expression levels by miRNAs may be a useful method to regulate HCCs during hepatitis viral infection.

Hepatocellular carcinoma (HCC) is the third most common cause of cancer-related mortality worldwide[1]. Although multiple major risk factors have been identified, such as genetic factors, environmental toxins, alcohol abuse, obesity, and metabolic disorders[2], infection with hepatitis virus B (HBV) or C (HCV) remains the major etiological factor for HCC[1].

Disease progression in HBV-induced or HCV-induced HCC is a multistep phenomenon. The clinical outcomes vary among individuals[1,3,4] because disease progression is influenced by both environmental and genetic risk factors. In terms of genetic susceptibility factors for HCV-induced HCC, we previously identified a single nucleotide polymorphism (SNP) site in the 5′-flanking region of the MICA gene on 6p21.33 (rs2596452) that is strongly associated with progression from chronic hepatitis C to HCC[5]. Individuals with the risk allele A of rs2596452 showed lower serum MICA protein levels[5]. Our subsequent study revealed that the same SNP site was also significantly associated with the risk of HBV-induced HCC[6]. However, interestingly, the risk allele was G in cases of HBV infection, which differed from HCV infection, and the individuals with the risk allele showed increased MICA protein expression levels[6]. Despite the different risk alleles at the same SNP site and inverse association between serum MICA levels and HCC risks in these two etiologies, MICA protein expression levels are significantly associated with susceptibility to HCC in chronic hepatitis viral infection.

MICA is highly expressed on viral-infected and cancer cells and acts as a ligand for NKG2D to activate the antitumor effects of natural killer cells and CD8 T cells[7,8]. This NKG2D-mediated tumor rejection is considered to be effective in the early stages of tumor growth[9–11]. Thus, the expression levels of MICA on the tumor cell surface may determine the antitumor efficacy, and the levels of shedding MICA in serum may act as a decoy of NKG2D to avoid tumor rejection.

Although several stress pathways regulate the transcription of the MICA gene[12,13], cellular microRNAs are suggested to control MICA protein expression via post-transcriptional mechanisms[14,15]. Recently, nucleic-acid-mediated gene therapy has been undergoing clinical trials[16]. Therefore, to target the clinical application of our GWAS results toward prevention of chronic-hepatitis-infection-induced HCC by nucleic-acid-mediated therapy, we determined the regulatory mechanisms of MICA protein expression using miRNA overexpression and miRNA functional silencing.

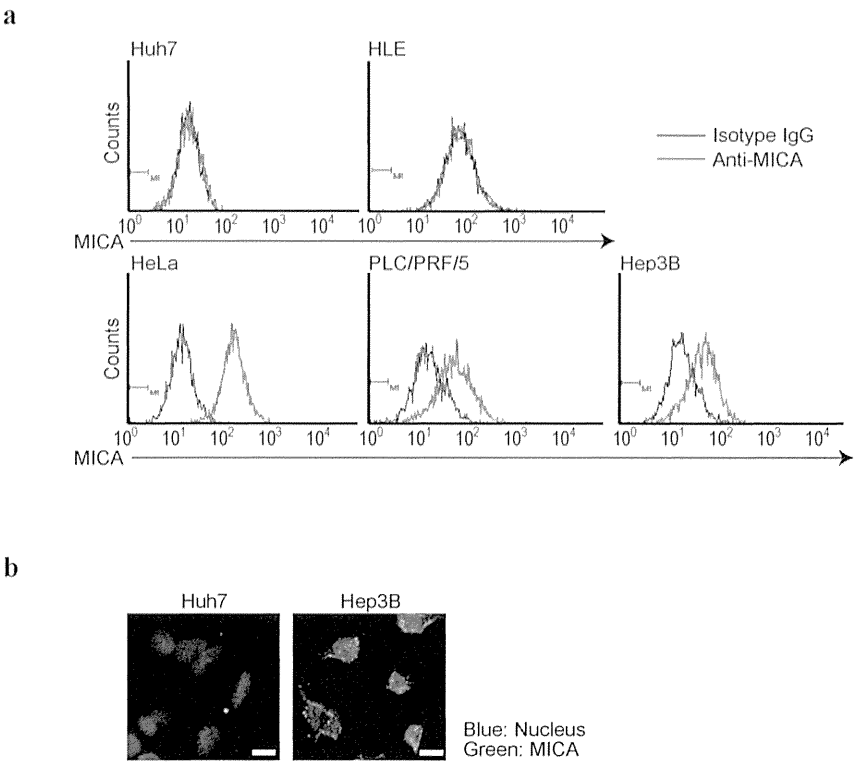

Figure 1 | Expression of MICA protein in HCC cells. (a), Flow cytometry assessment of MICA protein expression in HCC cells (purple lines). Isotype IgG was used for background staining (black lines). HeLa cells were used as the positive control. Representative results from two independent experiments are shown. (b), Immunofluorescence staining for MICA in Huh7 and Hep3B cells. Representative images from two independent experiments are shown. Scale bar, 25 μm.

Results

HCC cell lines differentially express MICA protein. To determine MICA protein levels in HCC cells, four representative HCC cell lines (Huh7, HLE, PLC/PRF/5, and Hep3B cells) underwent flow cytometry to evaluate MICA protein expression because no appropriate antibodies against MICA protein are at present available for western blotting. HeLa cells, which are known to express MICA protein[17], were used as a positive control. Hep3B and PLC/PRF/5 cells expressed substantial MICA protein levels, Huh7 and HLE cells expressed no MICA protein (Figure 1a). This was confirmed by immunocytochemistry using Huh7 and Hep3B cells, which showed staining mainly of cell surfaces (Figure 1b). These results suggest that the MICA protein expression status depends on the cell line examined, even those from the same organ.

The MiR25-93-106b cluster regulates MICA expression. Because upregulation of MICA expression was observed in Dicer-knockdown cells[18], we hypothesized that MICA expression levels may be at least partly regulated by miRNAs. We initially tested miRNAs that might affect MICA expression using reporter constructs into which MICA 3′-untranslated region (3′UTR) sequences were cloned and by transiently overexpressing 76 mature synthetic microRNAs, which were selected on the basis of their hepatic expression level, as in our previous studies[19,20]. Among the microRNAs examined, several may target MICA 3′UTR (Supplementary Figure 1). Among them, we focused on miR93 and miR106b, which were considered to target MICA 3′UTR based partly on the results of our initial miRNA testing described above; in addition, their possible target sequences were identified in the MICA 3′UTR sequences by a computational search using TargetScan 6.0 [21]. Additional reasons that we focused on these two miRNAs were as follows: 1) these miRNAs share the same seed sequences, to which two perfect-match complementary sequences exist in the 3′UTR of MICA (Figure 2a); 2) the target sequences are highly conserved among mammals and are thus likely to be biologically important sites; and 3) these miRNAs are located as a "miR25-93-106b cluster" on human chromosome 7q22.1, and so they may be expressed together under the same transcriptional control. We introduced mutations in the first possible miRNA target sequences of MICA 3′UTR in the reporter constructs (Supplementary Figure 2a); these sequences have a higher likelihood to be target sites, as determined by TargetScan. Co-transfection experiments revealed that reporter activity was suppressed by overexpression of a miR25-93-106b cluster-expressing plasmid (Figure 2b and Supplementary Figure 2b). The overexpression of an unrelated miR (let-7g)-expressing plasmid did not have any significant effects on the reporter activity (Supplementary Figure 2c) and the suppressive effect was lost using constructs with three point mutations in the seed sequences (Figure 2c), suggesting that miR25-93-106b directly targets these sequences and suppresses gene expression.

To confirm these effects, we generated HeLa and Hep3B cell lines that stably expressed the miR25-93-106b-cluster by transducing cells with miR25-93-106b-cluster-expressing lentiviruses (Figure 2d). As expected, the expression of the miR25-93-106b-cluster significantly suppressed MICA protein expression (Figure 2e). However, the expression levels of endogenous miR93 and 106b were not always proportional to the levels of MICA protein expression in the cell lines examined (Supplementary Figure 3). These results suggest that MICA protein expression can be regulated by miR93 and 106b, but that its expression is simultaneously endogenously regulated by other factors (possibly by promoter activities, including epigenetic changes).

Inhibition of miR25-93-106b function increases MICA protein expression. To develop methods of enhancing MICA protein expression levels based on the above results, we examined the

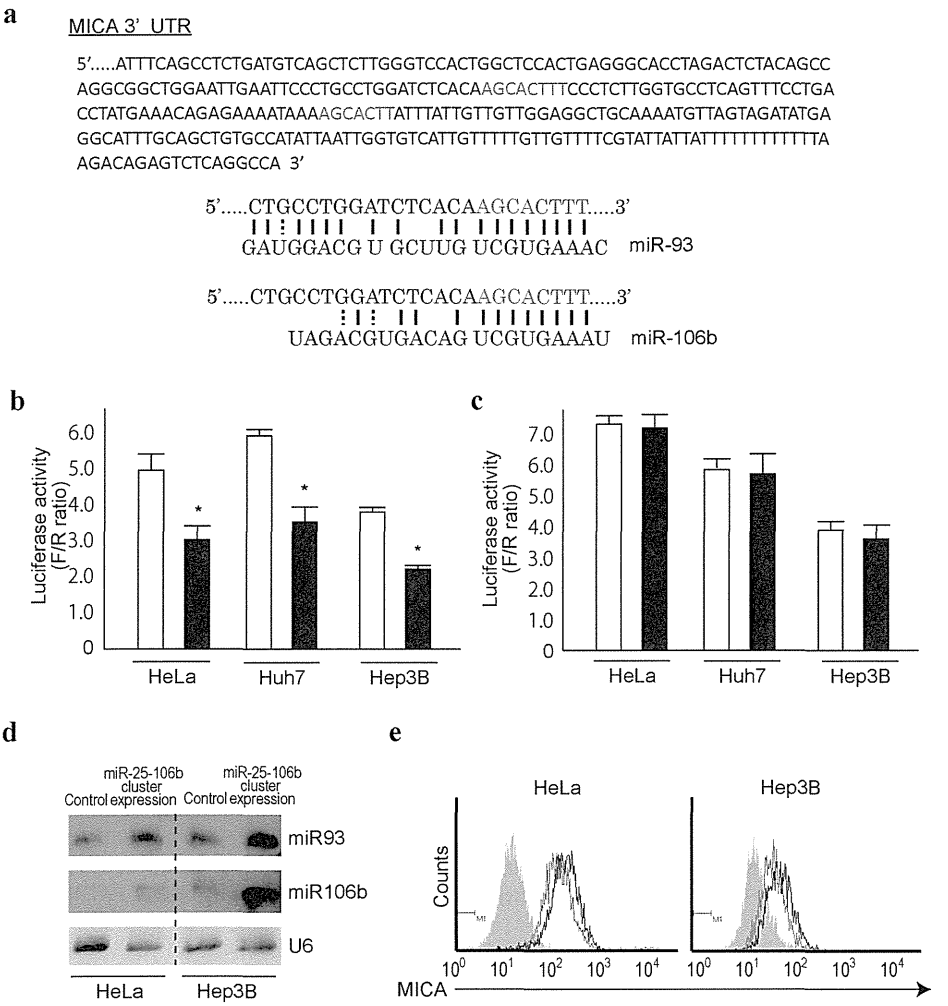

Figure 2 | miR93 and 106b target MICA 3′UTR. (a), Sequences of MICA 3′UTR (upper). Letters in red are the sequences completely matched with the seed regions of miR93 and 106b. The complementarities between the first predicted target in the MICA 3′UTR and miRNA sequences are shown below. (b), (c), Cells were co-transfected with pGL4-TK (renilla luciferase as an internal control), Luc-MICA-3′UTRwt (b) or Luc-MICA-3′UTRmut (c), and either an empty control vector (white bar) or miR25-93-106b-cluster expression plasmid (black bar). Data shows the means ± s.d. of the raw ratios (F/R) obtained by dividing firefly luciferase values with renilla luciferase values of three independent experiments. $*p < 0.05$. (d), miR93 and miR106b expression levels in control and stably miR25-93-106b cluster-expressing cells were determined by northern blotting. U6 levels were used as a loading control. Representative images from two independent experiments are shown. Full-length blot images are available in Supplementary Figure 5. (e), Suppression of MICA expression by overexpression of miRNA93 and 106b. Flow cytometry assessment of MICA protein expression in control (black lines) and stably miR25-93-106b cluster-expressing HeLa and Hep3B cells (red lines). Gray-shaded histograms represent the background staining using isotype IgG. Representative results from two independent experiments are shown.

effects of functional downregulation of miR25-93-106b on MICA expression. We first performed a reporter assay of transient functional silencing of miR25-93-106b using a construct that produces mature anti-sense RNAs designed to silence miR25-93-106b function. As expected, the reporter activities with MICA 3′UTR sequences were enhanced by the functional silencing of miR25-93-106b in HeLa, Hep3B, and Huh7 cells (Figure 3a). However, such effects were not observed using mutant reporter constructs not targeted by those miRNAs (Figure 3b), suggesting that the enhancing effects of the reporter activities were miRNA-dependent.

Next, HeLa, Hep3B, and Huh7 cells were stably transduced with a lentivirus that expresses anti-sense RNAs as described above, and MICA protein expression levels were determined by flow cytometry. Consistent with the reporter assay results, MICA protein expression was increased in HeLa and Hep3B cells by the functional silencing of miR25-93-106b (Figure 3c). However, in Huh7 cells, which express no MICA protein in the normal state, silencing of miR25-93-106b had no effect on MICA protein expression (Figure 3c). These results suggest that MICA protein expression levels can be regulated by modulating miRNA function, albeit only if at least a small quantity of MICA protein is present. In contrast, modulation of miRNA function does not influence MICA protein expression levels when the MICA protein is not expressed, but this could be because there are other forms of regulation at extremely low levels.

MICA protein levels are related to tumor susceptibility to NK cells. To determine the consequences of the modulation of MICA protein expression levels by miRNAs, we first determined the binding ability of NKG2D, a receptor of MICA, using HeLa and Hep3B cells overexpressing the miR25-93-106b cluster or with silencing of miR25-93-106b function. As expected, the levels of NKG2D binding to the cells, theoretically through binding to MICA, were decreased in HeLa and Hep3B cells overexpressing the miR25-93-106b cluster (Figure 4a). On the contrary, the levels of NKG2D binding to the cells were increased in HeLa and Hep3B cells in which miR25-93-106b function had been silenced (Figure 4b).

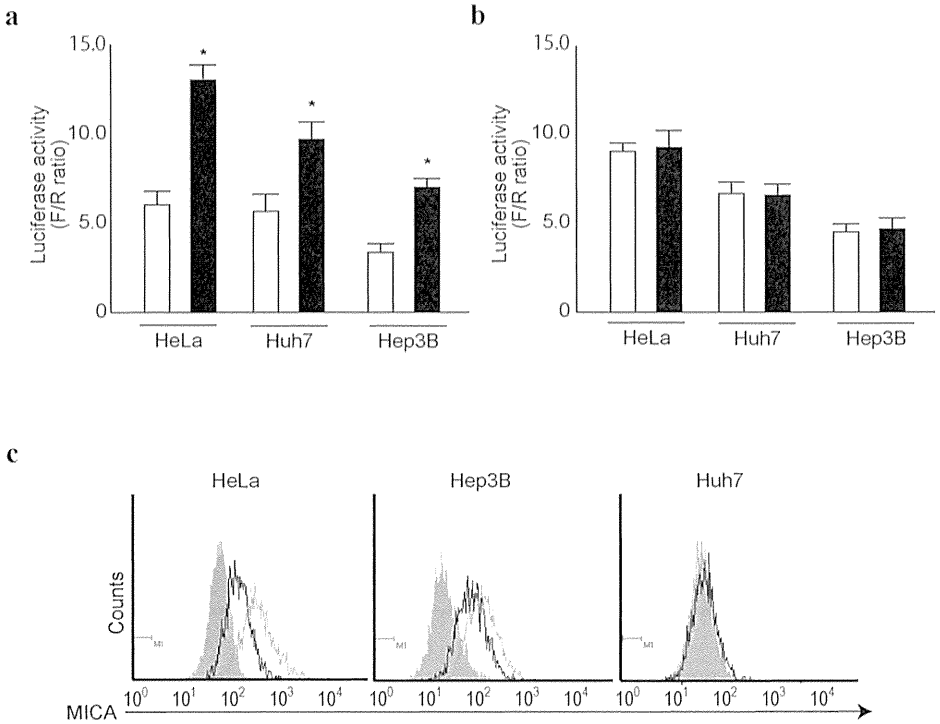

Figure 3 | Silencing of miR25-93-106b cluster enhances MICA expression. (a), (b), Cells were co-transfected with pGL4-TK (internal control), Luc-MICA-3′UTRwt (a) or Luc-MICA-3′UTRmut (b), and either an empty control vector (white bar) or plasmid expressing mature anti-sense sequences of miR25-93-106b cluster (black bar). Data shows the means ± s.d. of the raw ratios (F/R) obtained by dividing firefly luciferase values with renilla luciferase values of three independent experiments. $*p < 0.05$. (c), Enhancement of MICA expression by expression of anti-sense sequences of the miR25-93-106b cluster. Flow cytometry assessment of MICA protein expression in control (black lines) and stably mature anti-sense sequences of miR25-93-106b cluster-expressing cells (green lines). Gray-shaded histograms represent the background staining using isotype IgG. Representative results from three independent experiments are shown.

Next, to determine whether tumor cells with different miRNA-induced MICA protein expression levels exhibited differing susceptibilities to NK-cell-mediated killing *in vivo*, we performed a tumor-clearance assay that measures short-term *in vivo* killing by NK cells[22]. Hep3B control cells, Hep3B cells with miR25-93-106b cluster overexpression, or Hep3B cells with miR25-93-106b and HA-tagged MICA overexpression, labeled with fluorescent DiO, were injected into C57Black6/J mouse tail veins together with an equal number of HeLa cells labeled with Dil (internal reference control). After 5 h, surviving Hep3B and HeLa cells in the lungs were enumerated by flow cytometry. The number of Hep3B cells that had survived divided by the number of HeLa cells that had survived represents the relative killing of Hep3B cells *in vivo*. As shown by the *in vitro* binding assay using NKG2D, the killing rate of Hep3B cells in which miRNA function had been silenced was higher, and that of cells overexpressing miRNAs was lower, than that of control cells. The effects of miRNA overexpression were similar to those obtained in MICA knocked-down Hep3B cells (supplementary Figure 4). Additionally, the lower cell-killing rate in Hep3B cells overexpressing miRNA was antagonized by the co-expression of exogenous MICA protein (Figure 4c), suggesting that the decreased clearance was mediated by reduced MICA expression levels secondary to overexpression of miRNAs. These results suggest that tumor progression and invasion can be regulated by expression or silencing of miRNAs in at least some cells by regulation of MICA expression levels.

Discussion

In this study, we showed that the miR25-93-106b cluster modulates MICA protein expression by HCC cells. Because our previous GWAS analyses identified that MICA is the critical gene determining HCC susceptibility in patients with chronic hepatitis infection[5,6], the herein-described methods of modulating MICA expression may be useful for developing novel methods of prevention and therapeutics against HCCs.

MICA is a membrane protein that acts as a ligand for NKG2D to activate innate anti-tumor effects through natural killer and $CD8^+$ cells[7]. Our previous GWAS study showed that a risk allele at the SNP in the MICA promoter region was significantly associated with the susceptibility of HCV-induced HCC as well as with lower serum MICA levels. Although polymorphisms at the same SNP site were also associated with HBV-induced HCC, the risk allele determining the susceptibility of HCC was somehow different from that in HCV-induced HCC. While the reason why different MICA gene variations act as risk alleles at the same SNP site between HBV- and HCV-induced HCC has not been elucidated, it is assumed that changes in the membrane-bound MICA and soluble MICA levels due to differences in post-translational processing according to virus type may affect the risk allele results. In any case, because the importance of the regulation of MICA expression levels to prevent development of HCC due to chronic hepatitis viral infection cannot be denied, the regulation of MICA levels by microRNAs as shown here may be useful for the development of preventive methods of preventing HCC development during chronic hepatitis infection.

While several cellular signaling pathways lead to upregulation of MICA[12,13], we used microRNAs to regulate the expression levels of MICA in this study. As shown by the results of our GWAS analyses, which found that the polymorphisms in the promoter region of MICA are associated with changes in the sMICA levels[5,6], promoter activities of the MICA gene also have significant effects on MICA expression levels[23]. Our results showed that miR93 and 106b expression levels were not always correlated with those of MICA in HCC cell lines, suggesting that the regulation of MICA expression is not solely

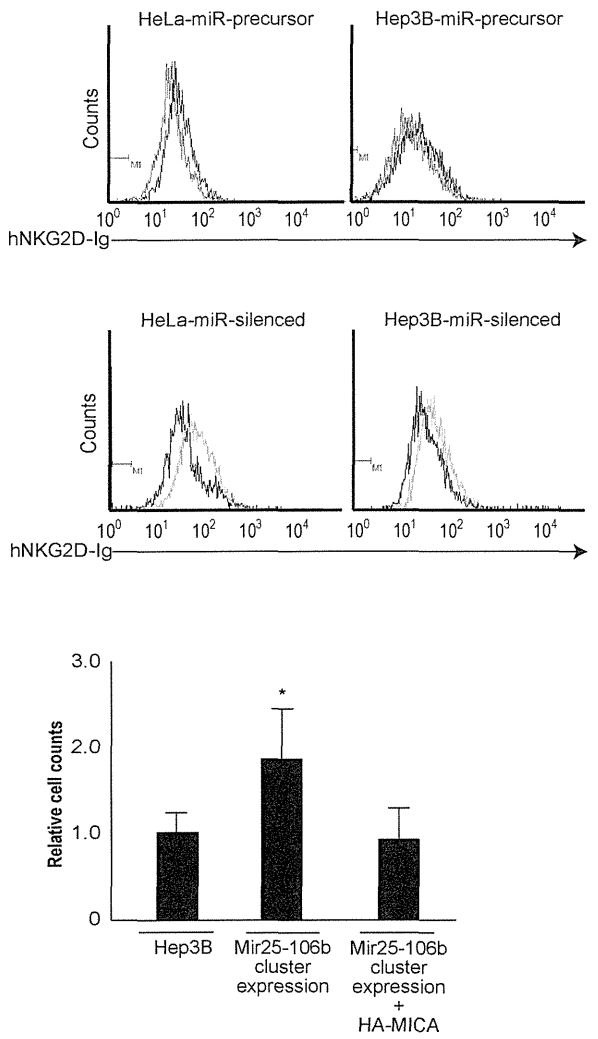

Figure 4 | NKG2D binding levels change in proportion to MICA expression levels. (a), (b), Flow cytometry of human IgG-fused NKG2D binding to the control (black lines), miR25-93-106b cluster-expressing cells (red lines) (a), and mature anti-sense sequences of miR25-93-106b cluster-expressing cells (green lines) (b). Representative results from three independent experiments are shown. (c), *In vivo* killing of DiO-labeled Hep3B and Dil-labeled HeLa cells (internal control cells) injected together into the tail veins of six mice in each group. Fluorescence intensities were quantified by flow cytometry as the ratio of Hep3B to HeLa cells in the lungs. The data from control Hep3B cells were set as 1.0. Data represent the means ± s.d. of three independent experiments. $*p < 0.05$.

dependent on miRNAs. In addition, in cells with no endogenous MICA expression, such as Huh7 cells, modulation of microRNA expression had no effect on the regulation of MICA expression. This suggests that at least low-level endogenous expression, which may be determined by promoter activities, are needed for regulation by miRNA. Therefore, changes in promoter activities and epigenetic changes in the MICA gene should also be determined. This will facilitate application of the regulatory function of miRNAs reported here.

One class of antisense oligonucleotides, namely locked nucleic acids, can be used to sequester microRNAs in the liver of various animals, including humans[16,24,25]. A clinical trial targeting miR-122 with the anti-miR-122 oligonucleotides miravirsen, the first miRNA-targeted drug, is underway for the treatment of HCV infection[16]. Thus, nucleic-acid-mediated gene therapy is becoming a realistic option. Modulation of MICA expression levels by such nucleic-acid-mediated therapy based on the results presented herein may also be a promising option for prevention and/or therapy of HCC.

In summary, we have shown that the miR25-93-106b cluster can be used to modulate MICA expression levels in HCC cells. Based on our GWAS results and associated studies, regulation of MICA protein expression levels is crucial to prevent the development of HCC during chronic hepatitis viral infection. It is important to identify the other factors that regulate MICA transcriptional activities as well as the post-translational processes and their association with susceptibility to HCCs. That said, miRNA regulation of MICA expression as shown here may facilitate regulation of the host innate immune system in an HCC-suppressive manner during chronic hepatitis viral infection.

Methods

Cell culture. The human HCC cell lines Huh7, HLE, PLC/PRF/5, and Hep3B were obtained from the Japanese Collection of Research Bioresources (JCRB, Osaka, Japan). The human cervical cancer cell line HeLa was obtained from the American Type Culture Collection (ATCC, Rockville, MD). All cells were maintained in Dulbecco's modified Eagle's medium supplemented with 10% fetal bovine serum.

Mouse. Experimental protocols were approved by the Ethics Committee for Animal Experimentation at the Graduate School of Medicine, the University of Tokyo and the Institute for Adult Disease, Asahi Life Foundation, Japan and conducted in accordance with the Guidelines for the Care and Use of Laboratory Animals of the Department of Medicine, the University of Tokyo, and the Institute for Adult Disease, Asahi Life Foundation.

Flow cytometry. Cells were hybridized with anti-MICA (1 : 500; R&D Systems, Minneapolis, MN) and isotype control IgG (1 : 500; R&D Systems) in 5% BSA/1% sodium azide/PBS for 1 h at 4°C. After washing, cells were incubated with goat anti-mouse Alexa 488 (1 : 1000; Molecular Probes, Eugene, OR) for 30 min. Flow cytometry was performed and data analyzed using Guava Easy Cyte Plus (GE Healthcare, Little Chalfont, UK).

Reporter plasmid construction, transient transfections, and luciferase assays. The reporter plasmid for the analysis of the effects of miRNAs on MICA 3′UTR were constructed by subcloning the MICA 3′UTR sequences from pLightSwitch-MICA 3UTR (SwitchGear Genomics, Menlo Park, CA) into the pGL4.50 vector (Promega, Madison, WI) at the *FseI* site by the In-Fusion method (Clontech, Mountain View, CA) to insert the MICA 3′UTR sequences into the 3′-UTR of the firefly luciferase gene, which was under the control of the CMV promoter. The sequences of the primers were 5′-CTA GAG TCG GGG CGG CG GCC ATT TCA GCC TCT GAT GTC AGC-3′ and 5′-GTC TGC TCG AAG CGG CCG GCC TGG CCT GAG ACT CTG TCT TAA-3′. The resultant plasmid (Luc-MICA 3′UTRwt) was used as a template for the construction of mutant reporter plasmid (Luc-MICA 3′UTRmut), which carries three point mutations in the seed sequences of miR93 and 106b in the MICA 3′UTR, itself generated by a Quik Change II XL Site-directed Mutagenesis Kit (Stratagene, Heidelberg, Germany) according to the manufacturer's instructions. Transient transfection and reporter assays were performed as described previously[26].

Lentiviral constructs, viral production, and transduction. To generate a neomycin-resistant miR25-93-106b cluster-expressing lentiviral construct, copGFP in the pmiRNA25-93-106b cluster-expressing plasmid (System Biosciences, Mountain View, CA) was replaced with a neomycin resistant gene, which was subcloned from the pCDH-Neo vector (System Biosciences), at the *FseI* site. The primers used were 5′-GCT ACC GCT ACG AGG CCG GCC CAT GAT TGA ACA AGA TGG ATT GCA-3′ and 5′-TCG CCG ATC ACG CGG CCG GCC TCA GAA GAA CTC GTC AAG AAG GC-3′. To remove the copGFP region from pmiRZIP25-93-106b (System Biosciences), a construct expressing mature anti-sense sequences of the miR25-93-106b cluster, sequences coding the GFP gene were removed by excision with *XbaI* and *PstI* sites followed by connecting the cut ends with annealed oligonucleotides (5′-CTA GAC GCC ACC ATG CTG CA-3′ and 5′-GCA TGG TGG CGT-3′) to maintain the coding frame and the expression of the downstream puromycin-resistance gene. To generate HA-tagged MICA protein overexpressing the lentiviral construct, MICA cDNA was amplified by PCR using a Halo-tag-MICA–expressing plasmid (Promega, Madison, WI) as a template and cloned into a pCDH-puro vector (System Biosciences) at the *NotI* site. The primer sequences used were 5′-ATC GGA TCC GCG GCC GCA CCA TGT ACC CAT ACG ATG TTC CAG ATT ACG CTA TGG GGC TGG GCC CGG TC-3′ and 5′-AGA TCC TTC GCG GCC GCT TAG GCG CCC TCA GTG GAG C-3′. Let-7g precursor expressing plasmid was generated by inserting about 1,000 bp long PCR product around the let-7g genomic region into pCDH-puro vector using *Xba*1 and *Not*1 sites. The production and concentration of lentiviral particles were described previously[27]. shRNA against MICA-producing lentiviral particles with puromycin resistant gene were purchased from SantaCruz Biotechnology (sc-4924-V, Dallas, TX). Cells were transduced with lentiviruses using

polybrene (EMD Millipore, Billerica, MA). The selections were performed with 400 μg/mL G418 and 2 μg/mL (HeLa) or 6 μg/mL (Hep3B) puromycin.

Immunocytochemistry. Cells on two-well chamber slides were fixed with 4% paraformaldehyde. Fixed cells were probed with the primary MICA antibody (R&D Systems) for 1 h after blocking with 5% normal goat serum for 30 min. Cells probed with the MICA antibody were incubated with the secondary Alexa Fluor 488 goat anti-mouse antibody (Molecular Probes) for 30 min. Slides were mounted using VectaShield with DAPI (Vector Labs, Burlingame, CA).

Northern blotting of miRNAs. Northern blotting of miRNAs was performed as described previously[27]. Briefly, total RNA was extracted using TRIzol Reagent (Invitrogen, Carlsbad, CA) according to the manufacturer's instructions. Ten micrograms of RNA were resolved in denaturing 15% polyacrylamide gels containing 7 M urea in 1 × TBE and then transferred to a Hybond N+ membrane (GE Healthcare) in 0.25 × TBE. Membranes were UV-crosslinked and prehybridized in hybridization buffer. Hybridization was performed overnight at 42°C in ULTRAhyb-Oligo Buffer (Ambion) containing a biotinylated probe specific for miR93 (cta cct gca cga aca gca ctt tg) and 106b (atc tgc act gtc agc act tta), which had previously been heated to 95°C for 2 min. Membranes were washed at 42°C in 2 × SSC containing 0.1% SDS, and the bound probe was visualized using a BrightStar BioDetect Kit (Ambion). Blots were stripped by boiling in a solution containing 0.1% SDS and 5 mM EDTA for 10 min prior to rehybridization with a U6 probe (cac gaa ttt gcg tgt cat cct t).

miRNA library screening. To screen for miRNAs that target MICA 3′-UTR, synthetic miRNA mimics and reporter constructs were used as described previously[19,20]. Seventy-six types of synthetic mature miRNAs that are highly expressed in the liver[28] were custom-made (B-Bridge, Tokyo, Japan) and transfected by RNAi Max (Life Technologies, Carlsbad, CA) into Huh7 cells in 96-well plates that had been transfected 24 h before with Luc-MICA 3′UTRwt. The cells were then incubated for another 24 h. As negative controls, oligonucleotides of artificial sequences were applied[19]. The luciferase activities were measured using a GloMax 96 Microplate Luminometer (Promega). The experiments were performed in duplicate.

NKG2D binding assay. Cells were incubated with 4 μg of recombinant human NKG2D fused to human IgG1 Fc chimera protein. After washing, cells were incubated with an Alexa488-conjugated affinity purified F(ab')2 fragment of goat anti-human IgG (Jackson ImmunoResearch Laboratories, West Grove, PA). As a negative control, cells were incubated with only Alexa488 anti-human IgG. The intensity of the fluorescence was determined by flow cytometry.

***In vivo* cell-killing assay.** Hep3B cells and HeLa cells were labeled with the fluorescent dye VybrantDiO and Dil (Molecular Probes), respectively. Cells were mixed at a density of 2×10^7 in 1-ml PBS, and 200 μl was injected into the tail vein. Five hours later, lungs were collected, and single-cell suspensions were collected using a cell strainer. Fluorescence was assayed by flow cytometry, and the ratio of the experimental Hep3B cells to HeLa cells (internal control) was calculated.

Statistical analysis. Statistically significant differences between groups were determined using Student's *t*-test when variances were equal. When variances were unequal, Welch's *t*-test was used instead. *P*-values of < 0.05 were considered to indicate statistical significance.

1. El-Serag, H. B. Epidemiology of viral hepatitis and hepatocellular carcinoma. *Gastroenterology* **142**, 1264–1273 (2012).
2. Sherman, M. Hepatocellular carcinoma: New and emerging risks. *Dig Liver Dis* **42**, S215–222 (2010).
3. Arzumanyan, A., Reis, H. M. & Feitelson, M. A. Pathogenic mechanisms in HBV- and HCV-associated hepatocellular carcinoma. *Nat Rev Cancer* **13**, 123–135 (2013).
4. Urabe, Y. *et al.* A genome-wide association study of HCV-induced liver cirrhosis in the Japanese population identifies novel susceptibility loci at the MHC region. *J Hepatol* (2013).
5. Kumar, V. *et al.* Genome-wide association study identifies a susceptibility locus for HCV-induced hepatocellular carcinoma. *Nat Genet* **43**, 455–458 (2011).
6. Kumar, V. *et al.* Soluble MICA and a MICA variation as possible prognostic biomarkers for HBV-induced hepatocellular carcinoma. *PLoS One* **7**, e44743 (2012).
7. Maccalli, C., Scaramuzza, S. & Parmiani, G. TNK cells (NKG2D+ CD8+ or CD4+ T lymphocytes) in the control of human tumors. *Cancer Immunol Immunother* **58**, 801–808 (2009).
8. Jinushi, M. *et al.* Impairment of natural killer cell and dendritic cell functions by the soluble form of MHC class I-related chain A in advanced human hepatocellular carcinomas. *J Hepatol* **43**, 1013–1020 (2005).
9. Diefenbach, A., Jensen, E. R., Jamieson, A. M. & Raulet, D. H. Rae1 and H60 ligands of the NKG2D receptor stimulate tumour immunity. *Nature* **413**, 165–171 (2001).
10. Hayakawa, Y. Targeting NKG2D in tumor surveillance. *Expert Opin Ther Targets* **16**, 587–599 (2012).
11. Guerra, N. *et al.* NKG2D-deficient mice are defective in tumor surveillance in models of spontaneous malignancy. *Immunity* **28**, 571–580 (2008).
12. Bauer, S. *et al.* Activation of NK cells and T cells by NKG2D, a receptor for stress-inducible MICA. *Science* **285**, 727–729 (1999).
13. Eleme, K. *et al.* Cell surface organization of stress-inducible proteins ULBP and MICA that stimulate human NK cells and T cells via NKG2D. *J Exp Med* **199**, 1005–1010 (2004).
14. Yadav, D., Ngolab, J., Lim, R. S., Krishnamurthy, S. & Bui, J. D. Cutting edge: down-regulation of MHC class I-related chain A on tumor cells by IFN-gamma-induced microRNA. *J Immunol* **182**, 39–43 (2009).
15. Stern-Ginossar, N. & Mandelboim, O. An integrated view of the regulation of NKG2D ligands. *Immunology* **128**, 1–6 (2009).
16. Janssen, H. L. *et al.* Treatment of HCV Infection by Targeting MicroRNA. *N Engl J Med* **368**, 1685–94 (2013).
17. Salih, H. R., Rammensee, H. G. & Steinle, A. Cutting edge: down-regulation of MICA on human tumors by proteolytic shedding. *J Immunol* **169**, 4098–4102 (2002).
18. Tang, K. F. *et al.* Decreased Dicer expression elicits DNA damage and up-regulation of MICA and MICB. *J Cell Biol* **182**, 233–239 (2008).
19. Takata, A. *et al.* MicroRNA-22 and microRNA-140 suppress NF-κB activity by regulating the expression of NF-κB coactivators. *Biochem Biophys Res Commun* **411**, 826–831 (2011).
20. Yoshikawa, T. *et al.* Silencing of microRNA-122 enhances interferon-a signaling in the liver through regulating SOCS3 promoter methylation. *Sci. Rep.* **2**, 637 (2012).
21. Lewis, B. P., Burge, C. B. & Bartel, D. P. Conserved seed pairing, often flanked by adenosines, indicates that thousands of human genes are microRNA targets. *Cell* **120**, 15–20 (2005).
22. Gazit, R. *et al.* Lethal influenza infection in the absence of the natural killer cell receptor gene Ncr1. *Nat Immunol* **7**, 517–523 (2006).
23. Lo, P. H. *et al.* Identification of a Functional Variant in the MICA Promoter Which Regulates MICA Expression and Increases HCV-Related Hepatocellular Carcinoma Risk. *PLoS One* **8**, e61279 (2013).
24. Lanford, R. E. *et al.* Therapeutic silencing of microRNA-122 in primates with chronic hepatitis C virus infection. *Science* **327**, 198–201 (2010).
25. Elmén, J. *et al.* LNA-mediated microRNA silencing in non-human primates. *Nature* **452**, 896–899 (2008).
26. Kojima, K. *et al.* MicroRNA122 is a key regulator of α-fetoprotein expression and influences the aggressiveness of hepatocellular carcinoma. *Nat Commun* **2**, 338 (2011).
27. Takata, A. *et al.* MicroRNA-140 acts as a liver tumor suppressor by controlling NF-κB activity by directly targeting DNA methyltransferase 1 (Dnmt1) expression. *Hepatology* **57**, 162–170 (2013).
28. Krützfeldt, J. *et al.* Silencing of microRNAs in vivo with 'antagomirs'. *Nature* **438**, 685–689 (2005).

Acknowledgments

This work was supported by Grants-in-Aid from the Ministry of Education, Culture, Sports, Science and Technology, Japan (#25293076, #25460979, and #24390183) (to M.Otsuka, Y.K. and K.K.), by Health Sciences Research Grants of The Ministry of Health, Labour and Welfare of Japan (to K.K.), and by grants from the Okinaka Memorial Institute for Medical Research, the Liver Forum in Kyoto, and the Princess Takamatsu Cancer Research Fund (to M.Otsuka).

Author contributions

T.K., M. Otsuka and K.K. planned the research and wrote the paper. T.K., M. Otsuka, T.Y., M. Ohno, A.T., C.S. and Y.K. performed the majority of the experiments. M.A. and H.Y. supported several experiments and analyzed the data. K.K. supervised the entire project.

Additional information

Supplementary information accompanies this paper at http://www.nature.com/scientificreports

Competing financial interests: The authors declare no competing financial interests.

How to cite this article: Kishikawa, T. *et al.* Regulation of the expression of the liver cancer susceptibility gene MICA by microRNAs. *Sci. Rep.* **3**, 2739; DOI:10.1038/srep02739 (2013).

The Oncogenic Role of Hepatitis C Virus

Kazuhiko Koike

Abstract

Persistent infection with hepatitis C virus (HCV) is a major risk toward development of hepatocellular carcinoma (HCC). However, it remains controversial in the pathogenesis of HCC associated with HCV whether the virus plays a direct or an indirect role. The observation that chronic hepatitis C patients with sustained high levels of serum alanine aminotransferase are prone to develop HCC suggests the significance of inflammation in hepatocarcinogenesis in hepatitis C. However, the rare development of HCC in patients with autoimmune hepatitis, which is accompanied by robust inflammation, even after the progress into cirrhosis, implies a possibility of the direct role of HCV in HCC development. What is the role of HCV, a simple plus-stranded RNA virus, whose genome is never integrated into the host genome, in hepatocarcinogenesis? The studies using transgenic mouse and cultured cell models, in which the HCV proteins are expressed, indicate the direct pathogenicity of HCV, including oncogenic activities. In particular, the core protein of HCV induces overproduction of oxidative stress by impairing the mitochondrial electron transfer system, through insulting the function of molecular chaperon, prohibitin. HCV also modulates the intracellular signaling pathways including mitogen-activated protein kinase, leading to the acquisition of growth advantage by hepatocytes. In addition, HCV induces disorders in lipid and glucose metabolisms, thereby accelerating the progression of liver fibrosis and HCC development. These results would provide a clue for further

K. Koike (✉)
Department of Gastroenterology, Graduate School of Medicine,
The University of Tokyo, Tokyo, Japan
e-mail: kkoike-tky@umin.ac.jp

M. H. Chang and K.-T. Jeang (eds.), *Viruses and Human Cancer*,
Recent Results in Cancer Research 193, DOI: 10.1007/978-3-642-38965-8_6,

understanding of the role of HCV in pathogenesis of persistent HCV infection including hepatocarcinogenesis.

Keywords
Hepatitis C · Hepatocellular carcinoma · Core protein · Oxidative stress · Lipid metabolism · Insulin resistance

Contents

1 Introduction

Worldwide, approximately 170 million people are persistently infected with hepatitis C virus (HCV), which induces a spectrum of chronic liver diseases, from chronic hepatitis, cirrhosis, eventually, to hepatocellular carcinoma (HCC) (Saito et al. 1990). HCV has been given an increasing attention because of its wide and deep penetration in the community, tied with a very high incidence of HCC in persistent HCV infection. Once liver cirrhosis is established in hosts persistently infected with HCV, HCC develops at a yearly rate of approximately 7 % (Ikeda et al. 1998), resulting in the development of HCC in nearly 90 % of HCV-associated cirrhotic patients in 15 years. In addition, the outstanding features in the mode of hepatocarcinogenesis in HCV infection, i.e., development of HCC in a multicentric fashion and in a very high incidence, are not common in other malignancies except for hereditary cancers such as familial polyposis of the colon. The knowledge on the mechanism underlying HCC development in persistent HCV infection, therefore, is imminently required for the prevention of HCC.

2 Hepatitis C Virus and Viral Proteins

The hepatitis C virus is an enveloped RNA virus belonging to the family *Flaviviridae*, and it contains a positive-sense, single-stranded RNA genome of approximately 9,600 nucleotides (nt) within the nucleocapsid (Houghton et al. 1991). The genome consists of a large open reading frame (ORF) encoding a

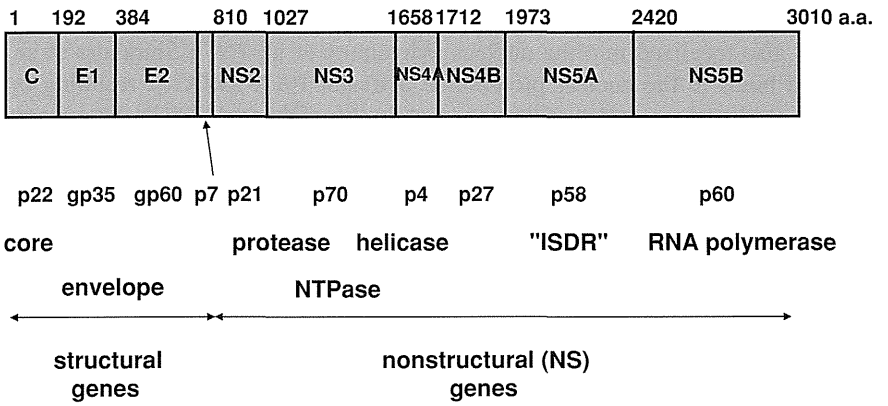

Fig. 1 The structure of hepatitis C virus genome. The HCV genome RNA encodes a polyprotein of 3,010 a.a., which is processed into structural and non-structural proteins by the cellular or viral proteases. One of the structural proteins, the core protein, shows a versatile character in experiments both in vitro and in vivo. ISDR, interferon sensitivity–determining region

polyprotein of approximately 3,010 amino acids (aa) (Fig. 1). The ORF is contiguous to highly conserved untranslated regions (UTRs) at both the 5' and 3' termini. The complete 5' UTR consists of 341 nt and acts as an internal ribosomal entry site. Such feature leads to the translation of the RNA genome using a cap-independent mechanism, rather than ribosome scanning from the 5' end of a capped molecule.

The polyprotein is processed by both the cellular and viral proteases to generate the viral gene products, which are subdivided into structural and non-structural proteins. The structural proteins, which are encoded by the NH_2-terminal quarter of the genome, include the core protein and the envelope proteins, E1 and E2. The E2 has an alternative form, E2-p7, though it is not clear whether or not the p7 composes the viral particle. The NS2, NS3, NS4A, NS4B, NS5A, and NS5B are the non-structural proteins that are coded in the remaining portion of the polyprotein. These include serine protease (NS3/4A), NTPase/helicase (NS3), and RNA-dependent RNA polymerase (NS5B).

The core protein of HCV occupies residues 1–191 of the precursor polyprotein and is cleaved between the core and E1 protein by host signal peptidase. The C-terminal membrane anchor of the core protein is further processed by host signal peptide peptidase (Moradpour et al. 2007). The mature core protein is estimated to consist of 177–179 amino acids and shares high homology among HCV genotypes. The HCV core protein possesses the hydrophilic N-terminal region "domain 1" (residues 1–117) followed by a hydrophobic region called "domain 2," which is located from residue 118–170. The domain 1 is rich in basic residues and is implicated in RNA binding and homo-oligomerization. The amphipathic helices I and II spanning from residue 119–136 and residue 148–164, respectively, in domain 2 are involved in the association of HCV core protein with lipid (Boulant et al. 2006). In addition, the region spanning from residue 112–152 is associated with membranes

of the endoplasmic reticulum and mitochondria (Suzuki et al. 2005). The core protein is also localized into the nucleus (Miyamoto et al. 2007; Shirakura et al. 2007) and binds to the nuclear proteasome activator PA28γ/REG γ, resulting in PA28γ-dependent degradation of the core protein (Moriishi et al. 2003). Autophagy is involved in the degradation of cellular organelles and the elimination of invasive microorganisms. Disruption of autophagy often leads to several protein deposition diseases. Recently, it has been shown that replication of HCV RNA induces autophagy in a strain-dependent manner, suggesting that HCV harnesses autophagy to circumvent cell death, and dysfunction of autophagy flux may participate in the genotype-specific pathogenesis of HCV (Taguwa et al. 2011).

3 Possible Role of HCV in Hepatocarcinogenesis

The mechanism underlying hepatocarcinogenesis in HCV infection is not fully understood yet, despite the fact that nearly 80 % of patients with HCC in Japan and 30 % of those in the world (Perz et al. 2006) are persistently infected with HCV (Kiyosawa et al. 1990; Saito et al. 1990; Yotsuyanagi et al. 2000). These lines of evidence prompted us to seek for determining the role of HCV in hepatocarcinogenesis. Inflammation induced by HCV should be considered in hepatitis viral infection: necrosis of hepatocytes due to chronic inflammation followed by regeneration enhances genetic aberrations in host cells, the accumulation of which culminates in HCC. This theory presupposes an indirect involvement of HCV in HCC via hepatic inflammation. However, this context leaves us with a serious question: Can inflammation alone result in the development of HCC in such a high incidence (90 % in 15 years) or multicentric nature in HCV infection?

The other role of HCV would have to be weighed against a rare occurrence of HCC in patients with autoimmune hepatitis in which severe inflammation in the liver persists, even after the development of cirrhosis. These backgrounds and reasonings lead to a possible activity of viral proteins for inducing neoplasia. This possibility has been evaluated by introducing genes of HCV into hepatocytes in culture with little success. One of the difficulties in using cultured cells is the carcinogenic capacity of HCV, if any, which would be weak and would take a long time to manifest itself. Actually, it takes 30–40 years for HCC to develop in individuals infected with HCV. On the basis of these viewpoints, investigation was started on carcinogenesis in chronic hepatitis C, in vivo, using transgenic mouse technology.

4 HCV Shows an In Vivo Oncogenic Activity in Mouse Studies

One of the major issues regarding the pathogenesis of HCV-associated liver lesion is whether the HCV proteins have direct effects on pathological phenotypes. Although several strategies have been used to characterize the hepatitis C viral

Table 1 Consequences of the expression of HCV proteins in mice

HCV gene	Genotype	Promoter	Protein expression	Phenotypes	References
Core	1b	HBV	Similar to patients	Steatosis, HCC, insulin resistance, oxidative stress	Moriya et al. (1997, 1998) Moriishi et al. (2003, 2007) Shintani et al. (2004) Miyamoto et al. (2007)
Core	1b	EF-1a	Similar to patients	Steatosis, adenoma, HCC, oxidative stress	Machida et al. (2006)
E1-E2	1b	HBV	Abundant	None in the liver	Koike et al. (1995, 1997)
Core-E1-E2	1b	Albumin	Similar to patients	Steatosis, HCC, oxidative stress	Lerat 2003
Core-E1-E2	1a	CMV	Similar to patients	Steatosis, HCC	Naas et al. (2005)
Structural proteins	1b	MHC	Low in the liver	Hepatitis	Honda et al. (1999)
Entire Polyprotein	1b	Albumin	Only mRNA detectable	Steatosis, HCC	Lerat 2003
Entire Polyprotein	1a	A1-antitrypsin		Steatosis, intrahepatic T-cell recruitment	Alonzi et al. (2004)
NS3/4A	1a	MUP		None (modulation of immunity)	Frelin et al. (2006)
NS5A	1a	ApoE		None (resistance to TNF)	Majumder et al. (2002)

HBV, hepatitis B virus; *EF*, elongation factor; *MUP*, major urinary protein; *Alb*, albumin; *CMV*, cytomegalovirus; *MHC*, major histocompatibility complex; *AT*, antitrypsin; *apo E*, apolipoprotein E

proteins, the relationship between the protein expression and disease phenotype has not been clarified. For this purpose, several lines of mice have been established which were transgenic for the HCV cDNA (Table 1). They include the ones carrying the entire coding region of HCV genome (Lerat et al. 2002), the core region only (Machida et al. 2006; Moriya et al. 1997), the envelope region only (Koike et al. 1995; Pasquinelli et al. 1997), the core and envelope regions (Lerat et al. 2002; Naas et al. 2005), and the core to NS2 regions (Wakita et al. 1998). Although detection of mRNA from the NS regions of the HCV cDNA has been reported (Honda et al. 1999; Lerat et al. 2002), the detection of HCV NS proteins in the transgenic mouse liver has not been successful. The reason for this failure in detecting NS proteins is unclear, but the expression of the NS enzymes may be harmful to mouse development and may allow the establishment of only low-expression mice.